sina-pub.ir

Punctuated Evolution of a Large Epithermal Province: The Hauraki Goldfield, New Zealand*

JEFFREY L. MAUK,[1,†] CHRIS M. HALL,[2] JOHN T. CHESLEY,[3] AND FERNANDO BARRA[3,**]

[1] *School of Environment, University of Auckland, Private Bag 92019, Auckland Mail Centre, Auckland 1142, New Zealand*

[2] *Department of Geological Sciences, University of Michigan, Ann Arbor, Michigan 48109-1005*

[3] *Department of Geosciences, University of Arizona, Tucson, Arizona 85721*

Abstract

The Hauraki goldfield in the Coromandel volcanic zone contains approximately 50 adularia-sericite epithermal Au-Ag deposits in a 200-km-long by 40-km-wide north-south–trending belt. These deposits have produced approximately 320,000 kg Au and 1.5 Mkg Ag and formed from Miocene to Pliocene subaerial hydrothermal systems. The goldfield has been divided into three provinces (northern, eastern, and southern), based on the host rocks and geologic setting of the deposits (Christie et al., 2007).

In the northern province of the goldfield, adularia from Paritu yields a single $^{40}Ar/^{39}Ar$ plateau date of 16.32 ± 0.13 Ma, and adularia from Opitonui yields a preferred $^{40}Ar/^{39}Ar$ age of 13.15 ± 0.03 Ma. Two Re-Os dates of molybdenite from porphyry-style mineralization at Ohio Creek overlap within error and yield dates of 11.87 ± 0.06 and 11.97± 0.08 Ma; geologic relationships suggest that this is the likely age of mineralization in the nearby Thames epithermal deposits.

In the eastern province, adularia from the Ohui deposit gives a preferred $^{40}Ar/^{39}Ar$ age of 8.29 ± 0.25 Ma, adularia from the Broken Hills deposit gives a preferred $^{40}Ar/^{39}Ar$ age of 7.12 ± 0.02 Ma, and adularia from the Wharekirauponga prospect yields a preferred $^{40}Ar/^{39}Ar$ age of 6.32 ± 0.12 Ma.

In the southern province, adularia from quartz veins at the Maratoto deposit provide a preferred $^{40}Ar/^{39}Ar$ age of 6.41 ± 0.04 Ma, and adularia from a quartz vein at the Sovereign deposit yields a preferred $^{40}Ar/^{39}Ar$ age of 6.70 ± 0.16 Ma. Two dates from vein adularia at the world-class Martha deposit overlap within error, and we interpret a preferred age for the deposit of 6.16 ± 0.06 Ma. Two samples of molybdenite from veins in the Martha deposit yield discrete Re-Os dates of 6.37 ± 0.03 and 6.51 ± 0.03 Ma. Adularia from one quartz vein from the Favona deposit yields a $^{40}Ar/^{39}Ar$ date of 6.05 ± 0.04 Ma. Host rock and vein adularia from the Karangahake deposit yield $^{40}Ar/^{39}Ar$ plateau dates that range from 6.90 ± 0.20 to 5.71 ± 0.13 Ma, which may reflect more than one stage of mineralization or protracted fluid flow. Adularia from veins at the Waiorongomai deposit yields a preferred $^{40}Ar/^{39}Ar$ age of 5.71 ± 0.03 Ma, and adularia from a vein at the Eliza deposit yields a preferred age of 4.47 ± 0.06 Ma. The southernmost deposit in the Hauraki goldfield, Muirs Reef, has adularia in quartz veins that yield $^{40}Ar/^{39}Ar$ plateaus dates of 2.12 ± 0.11 to 1.78 ± 0.16 Ma.

Combined with previous work, these results indicate that mineralization in the Hauraki goldfield ranges from 16.3 Ma in the north to 2 Ma in the south, and clusters into two distinct groups that correlate with location, volcanic stratigraphy, and mineralization style. The first group, from ~16.3 to ~10.8 Ma contains epithermal veins, including bonanza-style veins, and porphyry-style mineralization that formed in the northern province in an arc that was dominated by andesitic volcanism. The second period of mineralization occurs primarily from 6.9 to 6.0 Ma in the eastern and southern provinces, when precious metals were deposited into thicker colloform-crustiform banded veins that formed in extensional settings in an arc that was erupting bimodal andesite-rhyolite compositions. Therefore, even though volcanism in the Coromandel volcanic zone was active from 18 to 2 Ma, Au-Ag mineralization was focused into two discrete periods of this arc formation, and the style of mineralization changed through time, coinciding with a change in style of volcanism. In addition, while Hauraki goldfield mineralization discontinuously lasted more than 11 m.y., greater than 80 percent of the known gold endowment was deposited in a relatively brief 0.9 Ma window between 6.0 and 6.9 Ma. These changes through time likely reflect, at least in part, reorganization of the Miocene Northland and Colville volcanic arcs in the New Zealand region of the southwest Pacific.

Introduction

EPITHERMAL Au-Ag deposits form from hydrothermal systems that most commonly develop in active volcanic regions (e.g., Simmons et al., 2005). Epithermal provinces occur in remnant and active volcanic arcs worldwide, including the Great Basin of the western United States (e.g., John, 2001;

Saunders et al., 2008), the Mexico silver belt (e.g., Albinson et al., 2001), Japan (e.g., Hishikari: Izawa et al., 1990), the Patagonia province of Argentina (e.g., Sillitoe, 2008), and the Hauraki goldfield of New Zealand (e.g., Christie et al., 2007). Work in these, and in other epithermal provinces has focused mainly on descriptions of individual deposits, and yet few integrated studies have documented the temporal evolution of volcanic systems and the relationships between tectonics, volcanism, hydrothermal activity, and the formation of epithermal gold deposits. Here, we document the regional chronology of the Hauraki goldfield, providing new $^{40}Ar/^{39}Ar$ dates of hydro-

thermal adularia and Re-Os dates of molybdenite from veins. These methods provide precise and accurate dates, and this is the first published application of Re-Os dating in New Zealand. We combine these new and previously published data to (1) document the north to south advance of epithermal mineralization in the goldfield, (2) help constrain the duration of hydrothermal mineralization in the Waihi district, and (3) evaluate working hypotheses for the integrated tectonic, volcanic, and hydrothermal evolution of this important epithermal province. Available data demonstrate that although mineralization occurred discontinuously from about 16.3 to 2 Ma, most (~80%) of the known gold endowment was deposited in a relatively brief 0.9 Ma window between 7 and 6 Ma.

Regional Geology

In the last 25 m.y., the North Island of New Zealand has undergone a considerable shift in the locus of volcanism, from the north- to northwest-trending Northland arc between 25 and 15 Ma, to the Coromandel volcanic zone between 18 and 2 Ma, and then to the currently active northeast-striking Tonga-Kermadec-Taupo Volcanic Zone arc (Fig. 1; Adams et al., 1994; Ballance, 1999; Hayward et al., 2001; Carter et al., 2003; Briggs et al., 2005). Although there is wide consensus on this overall evolution, important details remain unclear, including the timing of the significant clockwise rotation of the arc from north-northwest to northeast trending.
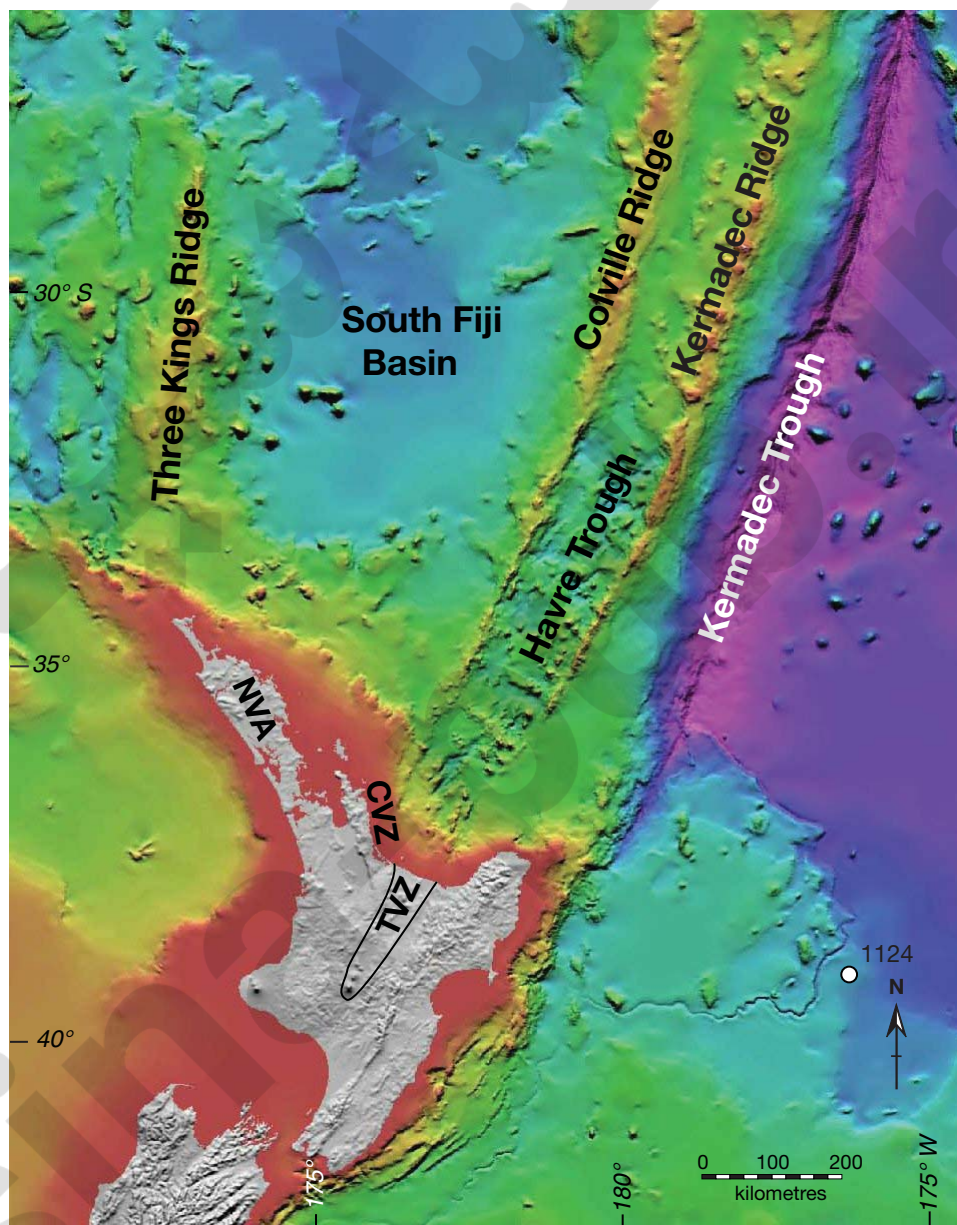

FIG. 1. Bathymetric and shaded digital elevation maps showing the location of volcanic arcs in the North Island of New Zealand. Bathymetric map of New Zealand's undersea topography from National Institute of Water and Atmospheric Research, New Zealand (CANZ, 1996). Abbreviations: CVZ = Coromandel volcanic zone, TVZ = Taupo Volcanic Zone, NVA = Northland volcanic arc, 1124 = Ocean Drilling Program (ODP) Leg 181 deep-ocean site 1124 from Carter et al. (2004).

The Hauraki goldfield contains approximately 50 adularia-sericite epithermal Au-Ag deposits that occur in a north-south–trending belt in the Coromandel volcanic zone, which follows the length of the Coromandel Peninsula (Fig. 2; Christie et al., 2007). Most orebodies consist of single to multiple quartz veins, and some deposits also had significant production from stockworks and/or hydrothermal breccias. Total production from 1862 through 2009 was 335,000 kg Au and 1.6 million kg Ag (Christie et al., 2007, and Newmont Waihi production records).

Jurassic graywacke and argillite of the Manaia Hill Group forms the basement of the region and is locally intruded by
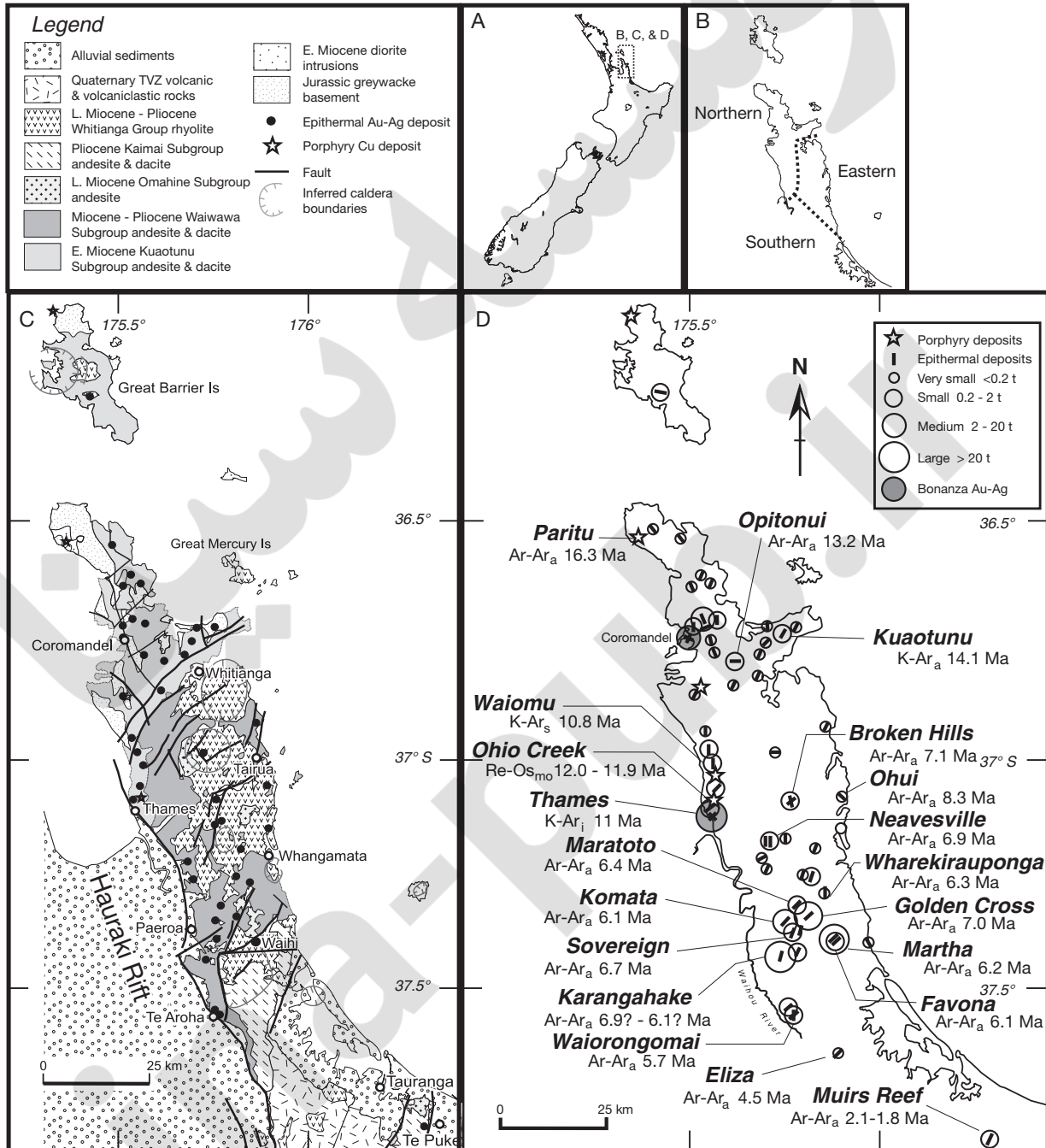

FIG. 2. A. Location of the Hauraki goldfield in the North Island of New Zealand. B. Location of the northern, eastern, and southern provinces of the Hauraki goldfield (from Christie et al., 2007). C. Geology of the Hauraki goldfield (from Christie et al., 2007). D. Location of mineral deposits in the Hauraki goldfield, vein orientations, past Au production, and ages of deposits (modified from Christie et al., 2007). The bar symbol shows the main strike of veins at each deposit. The K-Ar dates are from Skinner (1986), Hunt and Roddick (1992, 1993), Sinusat (1992), Adams et al. (1994), and Brathwaite and Christie (1996), whereas the $^{40}Ar/^{39}Ar$ and Re-Os dates are from Mauk and Hall (2004), and this publication. Subscripts show the mineral that was dated: a = adularia, i = illite, mo = molybdenite, s = sericite.

Late Miocene Coromandel Group dioritic intrusives (Skinner, 1972). The Manaia Hill Group is overlain by Miocene to Pliocene Coromandel Group andesite and dacite; this is subdivided into the Kuaotunu Subgroup, which formed in the northern part of the goldfield approximately 18 to 11 Ma, and the Waiwawa Subgroup, which formed in the southern and eastern part of the goldfield approximately 10 to 5.6 Ma (Edbrooke, 2001, and references therein). The southern goldfield also contains the 8.1 to 6.6 Ma Omahine Subgroup and the 5.6 to 3.8 Ma Kaimai Subgroup. Late Miocene to Pliocene (ca. 11-1.5 Ma) Whitianga Group rhyolites overlie and interfinger

with Coromandel Group rocks, and the volumetrically minor Mercury Basalts formed from 9.1 to 7.8 Ma and from 6.0 to 4.2 Ma (Skinner, 1986; Adams et al., 1994; Fig. 3). Lithology exerts a strong control on the location of orebodies; greater than 95 percent of Hauraki goldfield production was derived from veins hosted by andesite and dacite of the Coromandel Group, even though other units form nearly 40 percent of the rocks in the goldfield (Brathwaite et al., 2001a; Christie et al., 2007).

The Hauraki goldfield contains NNW- and NNE-striking faults and fractures with steep to moderate dips, which range
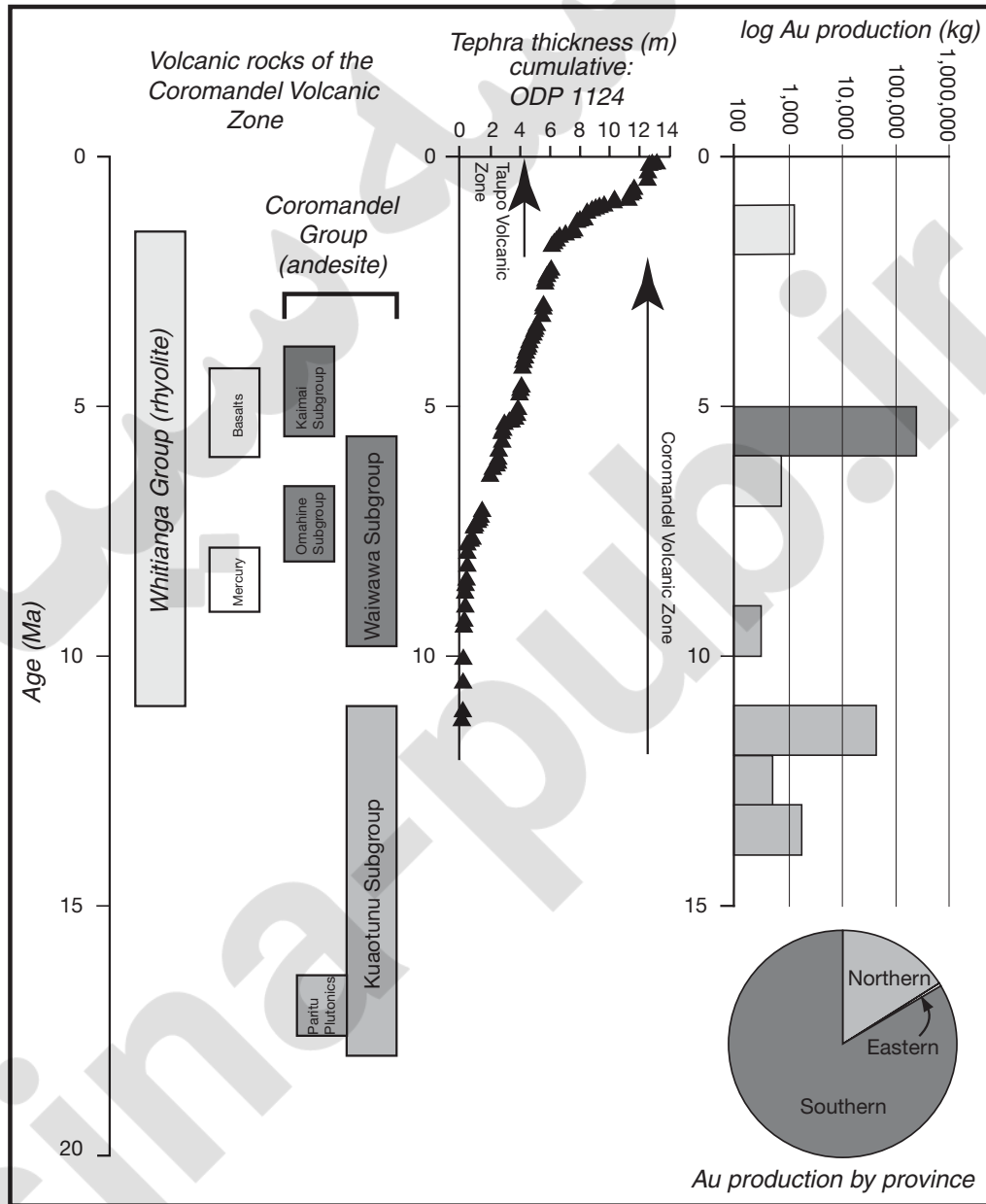

Fig. 3. Generalized stratigraphy of the Coromandel volcanic zone, showing volcanic units referred to in this text. Modified from Edbrooke (2001). Cumulative tephra thickness from drill core in Ocean Drilling Program (ODP) Leg 181 deepocean site 1124. Redrawn from Carter et al. (2003). Histogram showing log Au production (kg) for the Hauraki goldfield vs. date of the deposits. The deposit ages are placed into 1 Ma groupings, and the ages are based on data from this paper and other sources cited herein.

from regional scale to strike lengths of a few hundred meters (Spörli et al., 2006). The north-northwest–striking faults are equally downthrown to the east and west, but most north-northeast–striking faults are downthrown to the south (Skinner, 1986). This displacement has exposed the Jurassic basement in the northern portion of the Coromandel Peninsula, and exposes younger volcanic rocks to the south (Fig. 2C).

The currently active NNW-trending Hauraki Rift forms the western margin of the Coromandel volcanic zone. The bounding faults on the rift have offsets of up to 4 km, and the rift is filled with a sequence of sediments and volcanic flows (Hochstein et al., 1986; Hochstein and Ballance, 1993). The initiation of the Hauraki rift is poorly constrained and may have been around 7 Ma (Hochstein and Ballance, 1993). However, sedimentologic evidence indicates that there was no significant graben between the Hauraki goldfield and the west coast of New Zealand in the late Pliocene (ca 3–2 Ma), and the more recent volcanic record indicates that the main subsidence in the southern Hauraki rift occurred between 2.1 and 1.2 Ma (Briggs et al., 2005; Hayward et al., 2006).

Local Geology

We used $^{40}Ar/^{39}Ar$ and Re-Os geochronology to determine the dates of hydrothermal minerals from the Paritu, Opitonui, Ohio Creek, Ohui, Broken Hills, Wharekirauponga, Maratoto, Sovereign, Karangahake, Martha, Favona, Waiorongomai, Eliza, and Muirs Reef deposits, and this section describes the local geology of these deposits. Combined with our previous work at Neavesville, Golden Cross, and Komata (Mauk and Hall, 2004), we now have $^{40}Ar/^{39}Ar$ and Re-Os dates from deposits that have contributed more than 90 percent of the Au production of the Hauraki goldfield.

Porphyry Cu-style mineralization at Paritu in the northern Coromandel Peninsula is hosted by a small diorite to granodiorite pluton that intrudes the basement Manaia Hill Group and early to middle Miocene andesites. The porphyry Cu- style mineralization occurs around Ongohi Stream and consists of chalcopyrite with magnetite and pyrite in hydrothermally altered quartz diorite (Skinner, 1976; Brathwaite and Pirajno, 1993).

The Opitonui gold-silver epithermal deposit produced 512 kg Au and 457 kg Ag from electrum-bearing quartz veins that occur in Kuaotunu Group andesite. Mineralization occurs in north- and east-trending quartz veins (Christie et al., 2007).

The Ohio Creek porphyry Cu-Au-Mo prospect was drilled between 1978 and 1981, which outlined mineralization with 0.1 to 0.2 percent Cu, 0.2 to 0.4 ppm Au, and ≤0.01 percent Mo (Merchant, 1986). The porphyry prospect shows potassic, phyllic, and advanced argillic alteration, and spatial relationships indicate that mineralization at Ohio Creek is genetically related to epithermal mineralization in the nearby Thames district (Brathwaite et al., 2001b). The Thames district was the second largest Au producer in the Haruaki Goldfield, with production of 44,847 kg Au and 21,780 kg Ag from bonanza-style veins (Christie et al., 2007).

The Ohui deposit was worked between 1893 and 1910, with recorded production of 5 kg Au and 3 kg Ag (Christie et al., 2007). Mineralization occurs in Coromandel Group andesite and Whitianga Group rhyolite, although quartz veins are generally thicker in the andesite (Brathwaite et al., 2001a). The Ohui deposit lies at the northern end of the Karangahake-Ohui structural trend, a north-northeast–trending structural corridor that contains several epithermal deposits and prospects (Rabone, 1991); veins at Ohui strike both north-northeast and northwest (Brathwaite et al., 2001a; Fitzgerald et al., 2006). Colloform-banded vein textures and local sinter in the area suggest that the veins are high level; sulfide and ore minerals include pyrite, electrum, Ag-Se sulfides, native Ag, proustite, pyrargyrite, chalcopyrite, and marcasite (Fitzgerald et al., 2006).

The Broken Hills epithermal deposit produced 737 kg Au and 964 kg Ag from quartz veins and breccia pipes that cut rhyolite of the Whitianga Group. This production makes Broken Hills the second largest rhyolite-hosted Au producer in the Hauraki goldfield (Christie et al., 2007). Kinematic indicators show that quartz veins formed in an extensional environment, and ore shoots commonly strike north-south, whereas barren sections of the veins more commonly strike north-northwest (Nortje et al., 2006; Rabone, 2006a). Vein widths and grades can change by several orders of magnitude over 1 to 2 m along strike of the veins, and ore minerals include electrum, acanthite, aguilarite, and naumannite (Moore, 1979; Rabone, 2006a).

The Wharekirauponga epithermal gold-silver prospect is hosted by Whitianga Group flow-banded rhyolite and rhyolitic tuff, and an andesite dike; the prospect has virtually no historic production. The rhyolites occur in a north-northeast–trending graben, and mineralization occurs in sheeted to stockwork quartz veins and as disseminated mineralization. Most veins strike north-northwest or north-northeast, and ore minerals include electrum, chalcopyrite, and arsenopyrite (Rabone et al., 1989; Brathwaite et al., 2001a; Christie et al., 2006).

The Maratoto epithermal deposit produced 138 kg Au and 544 kg Ag from northeast-trending quartz veins with localized fan-shaped bonanza mineralization. Ore minerals include pyrite, marcasite, sphalerite, galena, chalcopyrite, acanthite, hessite, and electrum. The deposit occurs in highly altered andesites of the Waipupu Formation of the Coromandel Group (Main, 1979; Christie et al., 2007).

The Sovereign (formerly known as Maoriland) Au-Ag deposit in the southern Waitekauri valley produced 141 kg Au and 89 kg Ag; it occurs in intensely altered andesite, dacite breccias, and pyroclastic flows of the Waipupu Formation that show significant K metasomatism. Quartz veins follow a north-northeast-striking normal fault in a highly silicified dacitic tuff breccia (Haworth and Briggs, 2006; Grodzicki et al., 2007; Booden et al., 2011; Simpson and Mauk, 2011).

The Karangahake epithermal gold-silver deposit was the third largest Au producer in the Hauraki goldfield, with historic production of 29,425 kg Au and 97,290 kg Ag; recent exploration has identified a resource of 5,700 kg Au and 23,000 kg Ag (Stevens and Boswell, 2006). Mineralization occurs primarily in the Maria and Welcome and/or Crown veins, which are quartz veins that contain pyrite, chalcopyrite, electrum, acanthite, and local sphalerite and galena (Brathwaite, 1989; Mauk et al., 2006a). Karangahake produced Au ore over an anomalously large vertical extent of greater than 700 m. Productive veins strike north to north-northeast, fill extensional

fractures, and occur in andesite flows and flow breccias of the Waipupu Formation of the Coromandel Group. Veins continue upward into the overlying Whitianga Group rhyolite, where they break up into a stockwork that is too low grade to be economic (Brathwaite, 1989; Smith et al., 2003; Stevens and Boswell, 2006).

Through 2009, the Waihi (Martha) deposit produced 210,944 kg Au and 1,299,893 kg Ag (Lorrance Torckler, writ. commun., 2010); it has produced nearly 70 percent of the Au in the Hauraki goldfield (Christie et al., 2007). From 1883 through 1952, the deposit was worked as an underground mine that exploited several veins along a strike length of greater than 1.5 km and from a vertical extent of up to 575 m (Brathwaite and Faure, 2002). Since 1988, it has been worked as an open-pit mine with a planned length of 840 m, width of 575 m, and depth of 250 m, which exploits remnants of veins targeted by earlier mining, stope fill, vein breccias, and the abundant veins and veinlets that occur between the main veins (Brathwaite et al., 2006). The deposit shows distinct mineral zonation, with pyrite, chalcopyrite, acanthite, electrum, and minor sphalerite and galena at shallow to intermediate levels, and pyrite, sphalerite, and galena at depth. Veins occur in andesite and quartz andesite of the Waipupu Formation of the Coromandel Group (Brathwaite and Christie, 1996).

The Favona deposit is a recently discovered blind epithermal deposit that occurs approximately 2 km east of the Martha mine. When mining began in 2006, the deposit had reserves of 1.1 Mt at 10 ppm Au and 36 ppm Ag (Torckler et al., 2006). The deposit occurs in altered andesite of the Waipupu Formation of the Coromandel Group (Brathwaite and Christie, 1996; Simpson and Mauk, 2007). The ore consists of veins and vein breccias that strike north-northeast and formed in an extensional environment (Mortimer, 2009). Ore minerals include pyrite, chalcopyrite, acanthite, tetrahedrite, and electrum, as well as uncommon naummanite (Ag_2Se) and aguilerite (Ag_4SeS); sphalerite and galena are more abundant at depth (Mauk et al., 2006b).

The Waiorongomai deposit produced 885 kg Au and 1,259 kg Ag from a series of quartz veins that strike northeast; these splay off the north-striking, 5-km-long barren Big Buck Reef (Wellman, 1954; Bates, 1989; Christie et al., 2007). The veins occur in andesite of the Waipupu Formation of the Coromandel Group. Mineralized veins contain pyrite, chalcopyrite, galena, spahlerite, and electrum, and limited data suggest that base metal sulfides increase with depth (Bates, 1989; Christie et al., 2007).

The Eliza deposit contains a 1-m-wide quartz vein that strikes north-northeast, but this vein was not economic and recorded production was only 5 oz Au (Houghton and Cuthbertson, 1989).

From 1912 to 1922, the Muirs Reef mine exploited a north-northeast–striking, west-dipping colloform banded vein that typically ranges from 0.5 to 2 m thick. The vein occurs in predominantly andesitic host rocks that contain minor rhyolite units (Rabone, 2006b). It was mined along a strike length of approximately 300 m and downdip for approximately 100 m and yielded 1,299 kg Au and 385 kg Ag (Christie et al., 2007). The deposit is the southernmost in the Hauraki goldfield.

Materials and Methods

We analyzed adularia and molybdenite from 15 deposits in the Hauraki goldfield (Fig. 4; App; online digital supplement Table A1). Our primary intent is to provide a set of dates for epithermal deposits in the Hauraki goldfield on a regional scale, so we have analyzed a limited number of samples from a relatively large number of deposits.

Petrographic studies show that illite commonly replaces adularia in host rocks, whereas adularia in veins generally lacks illite (Fig. 4). Therefore, in most places we determined $^{40}Ar/^{39}Ar$ dates using adularia from veins (App.). The paragenetic sequence of vein minerals in various deposits has been summarized by other workers, and in the Hauraki goldfield, veins that contain adularia are commonly banded and contain electrum and various sulfide minerals as trace to minor phases intergrown with these banded veins (e.g., Simpson et al., 2001; Brathwaite and Faure, 2002; Begbie et al., 2007; Christie et al., 2007; Simpson and Mauk, 2007, 2011; Fig. 4). Therefore, the $^{40}Ar/^{39}Ar$ dates of vein adularia that we report here represent the age of mineralization of various deposits.

We analyzed adularia from veins and/or host rocks at 14 deposits in the Hauraki goldfield at the University of Michigan (Table 1; Apps. 1, 2). Some vein samples, such as those from Broken Hills, contain coarse-grained adularia crystals that were directly separated by handpicking. Adularia separates were obtained from other samples by heavy liquid separation followed by handpicking or by staining with sodium cobaltinitrite followed by handpicking. We quantified the amount of adularia in these separates by comparing X-ray diffraction (XRD) profiles of the separates to XRD profiles from a series of two-component mixtures with known concentrations of quartz and adularia. X-ray diffraction patterns were collected using a Philips PW 1050/25 diffractometer. Due to the fine-grained nature of the adularia and its common intergrowths with quartz, we could not obtain pure adularia separates for some samples. However, quartz was the only impurity that was identified by XRD analyses, and because it contains no potassium in its lattice, we conclude that it is not a source of contamination, only a dilutant. All samples have Auckland University (AU) numbers and are lodged in the collection of the Geology Department at the University of Auckland.

Samples for $^{40}Ar/^{39}Ar$ analysis from Martha and Favona were irradiated for 6 h in location L67 of the Phoenix-Ford Memorial Reactor at the University of Michigan, and samples from other deposits were irradiated in location 5C at the McMaster Nuclear Reactor, which is located on the campus of McMaster University, Hamilton, Ontario, Canada. Adularia was wrapped in pure aluminum foil and loaded into fused silica tubing for neutron irradiation. Samples were step-heated using the defocused beam from a 5-W argon-ion continuous laser, and analyses were carried out using a VG 1200S mass spectrometer equipped with a Daly detector operating in analog mode. The dates quoted are relative to an age of 27.99 Ma for standard biotite FCT-3, which in turn is relative to an age of 520.4 Ma for standard hornblende MMhb-1 (Hall and Farrell, 1995). The Ca interference corrections were $^{39}Ar/^{37}Ar = 1397$, $^{36}Ar/^{39}Ar = 0.421$, and the K correction was $^{40}Ar/^{39}Ar = 0.019$ for the Phoenix-Ford irradiation. The interference correction factors for the McMaster
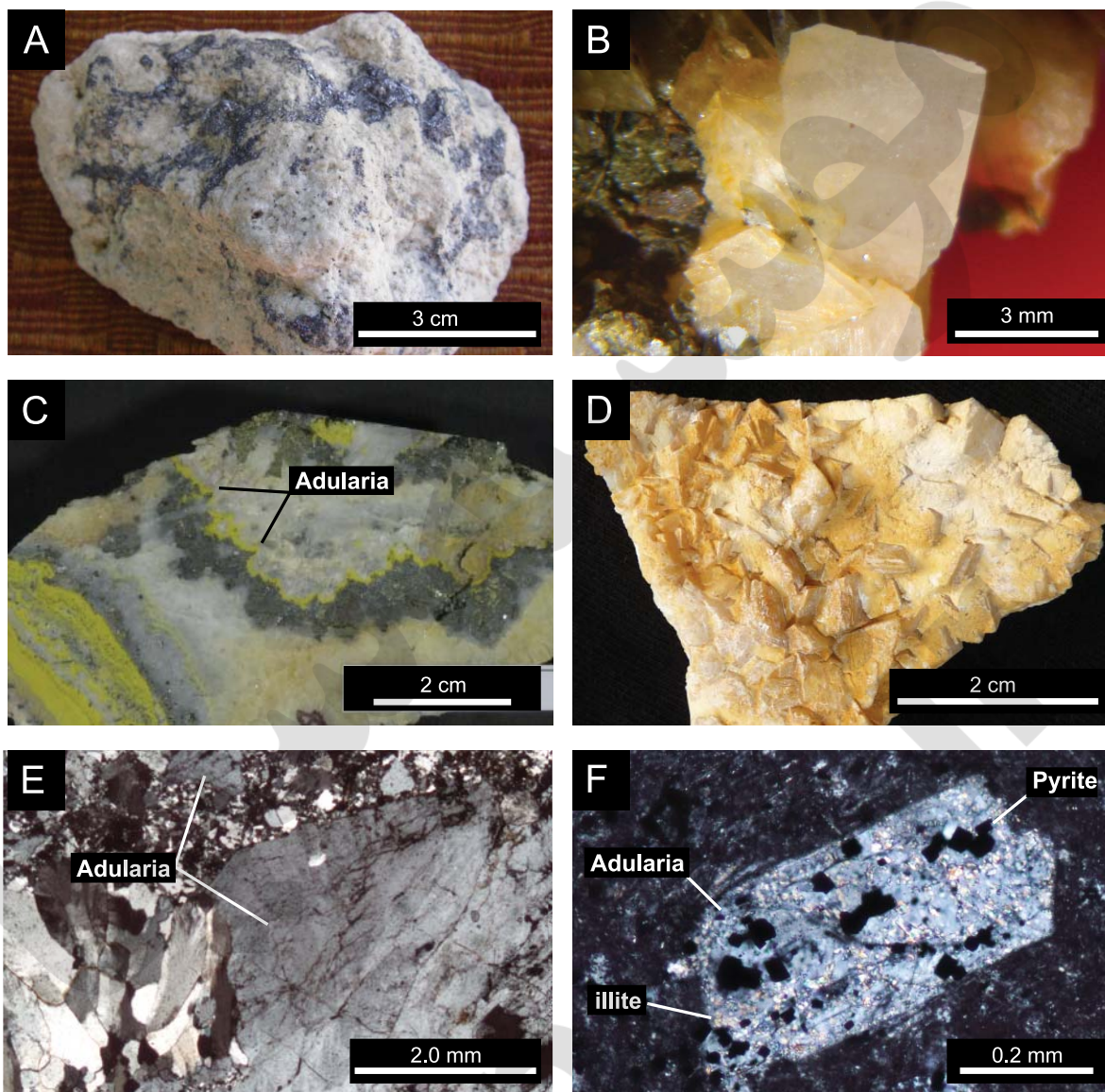
FIG. 4. Representative photographs of samples analyzed in this study. A. Molybdenite in quartz vein from the Martha mine. Sample AU 59725. B. Adularia from quartz vein at Paritu. Sample AU 56763. C. Banded quartz vein with adularia and base metal sulfides from the Waiorongomai deposit. The adularia has been stained yellow. Sample AU 33973. D. Coarse-grained adularia from the Broken Hills deposit. Sample AU 56756. E. Transmitted light photomicrograph showing adularia grains in a quartz vein from the Waiorongomai deposit. Sample AU 33870. F. Transmitted light photomicrograph showing porphyritic andesite host rock from the Karangahake deposit. Adularia has completely replaced plagioclase phenocrysts, and illite has partially replaced the adularia. Sample AU 57488.

irradiation were 1449, 0.425, and 0.037 for $^{39}Ar/^{37}ArCa$, $^{36}Ar/^{39}ArCa$, and $^{40}Ar/^{39}ArK$, respectively. The J values were calculated by interpolating a cosine function that was fitted through values measured from standards as a function of position within the irradiation can. Individual sample J value error estimates include measurement uncertainties from analyses of standards plus scatter of the standard values about the fitted J function. Mass discrimination was monitored daily, although the Baur-Signer source of the VG1200S does not exhibit rapid changes in mass discrimination. Over the past 3 yrs, the atmospheric $^{40}Ar/^{36}Ar$ ratio using the Faraday detector has been steady at ~301 and the ratio on the Daly detector has been ~290. All analyses were performed using the Daly detector and quoted isotope ratios and ages are corrected to for mass discrimination assuming an atmospheric $^{40}Ar/^{36}Ar$ ratio of 295.5.

Plateau dates were calculated as error weighted averages for adjacent gas fractions. A minimum of 50 percent of the ^{39}Ar was released within at least three successive steps to form a plateau, and the scatter about the error weighted average has a mean squared weighted deviate (MSWD) of no more than 2.0. If the MSWD is >1, the plateau date error is scaled up by multiplying by MSWD. The total gas date is calculated by adding up all the gas volumes and calculating a date from the derived isotope ratios. This date should be equivalent to a conventional K-Ar date.

TABLE 1. $^{40}\text{Ar}/^{39}\text{Ar}$ Age Determinations of Adularia from the Paritu, Opitonui, Broken Hills, Wharekirauponga, Maratoto, Sovereign, Waihi, Favona, Karangahake, and Waiorongomai Deposits (all errors are ±2σ)

AU no.	CM Hall no.	Location	Plateau	MSWD	F39 (%)	Isochron	40/36 Intercept	n	MSWD	Total gas	Comments
56756	MC07-S16a	Broken Hills	7.15 ± 0.05	0.94	100%	7.14 ± 0.06	296.2 ± 1.6	13	0.95	7.20 ± 0.14	Rhombohedral adularia crystals from vein
56756	MC07-S16b	Broken Hills	7.12 ± 0.06	1.16	100%	7.12 ± 0.06	296.3 ± 2.6	13	1.22	7.15 ± 0.10	Duplicate of above
56757	MC07-S17a	Broken Hills	7.12 ± 0.03	1.78	98.7%					7.12 ± 0.04	Rhombohedral adularia crystals from vein
56757	MC07-S17a	Broken Hills				7.08 ± 0.10	346.8 ± 148	9	1.84		Plateau points
56757	MC07-S17b	Broken Hills	7.12 ± 0.03	0.47	100%	7.12 ± 0.03	295.1 ± 5.8	13	0.51	7.12 ± 0.05	Duplicate of above
59722	MC24-m3a	Eliza	4.49 ± 0.12	0.34	85%	4.49 ± 0.12	304.3 ± 9.8	13	0.71	4.64 ± 0.23	Adularia from quartz vein
59722	MC24-m3a	Eliza				4.49 ± 0.20	288.8 ± 181	4	0.51		Plateau points
59722	MC24-m3b	Eliza	4.46 ± 0.07	0.5	98%	4.47 ± 0.07	277.3 ± 12	13	0.68	4.33 ± 0.13	Duplicate of above
59722	MC24-m3b	Eliza				4.47 ± 0.08	279.7 ± 71	7	0.51		Plateau points
55007	MI91-C26a	Favona	6.01 ± 0.14	0.96	59.8%					6.76 ± 0.13	Adularia from quartz vein
55007	MI91-C26b	Favona	6.07 ± 0.10	1.52	60.9%					6.52 ± 0.09	Duplicate of above
59720	MC24-m6a	Jubilee/Scotia	6.26 ± 0.07	1.47	100%	6.26 ± 0.08	296.2 ± 8.0	13	1.60	6.32 ± 0.10	1- to 2-mm-wide adularia veinlet
59720	MC24-m6b	Jubilee/Scotia	6.14 ± 0.06	1.70	100%	6.13 ± 0.06	297.7 ± 12	13	1.81	6.14 ± 0.07	Duplicate of above
43566	MC07-S28a	Karangahake	–							6.44 ± 0.07	Adularia from comb quartz vein
43566	MC07-S28b	Karangahake	6.40 ± 0.08	1.61	84.1%	6.29 ± 0.14	302.4 ± 8.6	13	1.86	6.47 ± 0.09	Duplicate of above
43566	MC07-S28b	Karangahake				6.28 ± 0.33	304.7 ± 24	8	1.70		Plateau points
43582	MC07-S27a	Karangahake	6.90 ± 0.20	1.17	76.9%					6.60 ± 0.23	White bluish, brecciated quartz vein
43582	MC07-S27a	Karangahake				6.54 ± 0.37	312.6 ± 15	9	0.50		Plateau points
43582	MC07-S27b	Karangahake	6.12 ± 0.23	1.13	59.4%					6.38 ± 0.21	Duplicate of above
43582	MC07-S27b	Karangahake				6.15 ± 0.27	292.5 ± 10	9	1.23		Plateau points
57488	MC07-S26a	Karangahake	5.75 ± 0.10	1.56	83.4%					5.59 ± 0.10	Host-rock adularia
57488	MC07-S26a	Karangahake				6.16 ± 0.41	280.3 ± 15	9	1.17		Plateau points
57488	MC07-S26b	Karangahake	5.71 ± 0.13	0.76	72.8%					5.61 ± 0.13	Duplicate of above
57488	MC07-S26b	Karangahake				5.81 ± 0.19	292.1 ± 5	8	0.58		Plateau points
18165	MC07-S14a	Maratoto	6.29 ± 0.08	0.55	55.3%	6.22 ± 0.08	306.4 ± 16	13	1.31	6.21 ± 0.08	Adularia in quartz vein
18165	MC07-S14a	Maratoto				6.22 ± 0.12	318.0 ± 42	4	0.16		Plateau points
18165	MC07-S14b	Maratoto	6.35 ± 0.10	1.17	93.7%	6.32 ± 0.12	301.0 ± 13	13	1.43	6.32 ± 0.12	Duplicate of above
18165	MC07-S14b	Maratoto				6.35 ± 0.16	295.3 ± 38	11	1.29		Plateau points
18172	MC07-S13a	Maratoto	6.44 ± 0.05	1.04	83.7%	6.47 ± 0.05	287.7 ± 1.4	13	0.83	6.08 ± 0.09	Coarse adularia in comb quartz vein
18172	MC07-S13a	Maratoto				6.50 ± 0.11	277.3 ± 29	10	1.01		Plateau points
18172	MC07-S13b	Maratoto	6.60 ± 0.07	0.91	63.6%	6.66 ± 0.15	284.2 ± 27	6	0.98	6.49 ± 0.07	Duplicate of above
18172	MC07-S13b	Maratoto				6.36 ± 0.09	249.5 ± 10	13	1.70		Plateau points
18176	MC07-S15a	Maratoto	6.37 ± 0.07	1.14	94.9%					6.34 ± 0.09	Coarse adularia intergrown with comb quartz in vein
18176	MC07-S15a	Maratoto				6.32 ± 0.12	312.1 ± 34	11	1.13		Plateau points
18176	MC07-S15b	Maratoto	6.43 ± 0.08	1.24	87.2%	6.41 ± 0.10	299.2 ± 7.2	13	1.77	6.42 ± 0.11	Duplicate of above
18176	MC07-S15b	Maratoto				6.47 ± 0.06	285.5 ± 72	10	1.39		Plateau points
46851	MI91-C21a	Martha				5.86 ± 0.31	296.0 ± 3.8	14	1.95	6.00 ± 0.39	Adularia from vein breccia
46851	MI91-C21b	Martha								6.43 ± 0.30	Duplicate of above
46876	MI91-C19a	Martha	6.17 ± 0.19	0.59	87.1%	6.03 ± 0.25	307.1 ± 12	14	0.90	6.38 ± 0.24	Host-rock adularia
46876	MI91-C19a	Martha								6.18 ± 0.19	Duplicate of above
55008	MI91-C20b	Martha	6.14 ± 0.04	1.17	99.8%	6.10 ± 0.04	299.4 ± 2.8	8	1.20	6.17 ± 0.05	Coarse adularia crystals in vein
55008	MI91-C20c	Martha	6.20 ± 0.07	1.22	92.0%	6.18 ± 0.08	297.3 ± 7.8	8	1.70	6.23 ± 0.08	Duplicate of above
55009	MI91-C25a	Martha	6.05 ± 0.12	0.84	70.9%					6.32 ± 0.19	Host-rock adularia
55009	MI91-C25b	Martha	6.09 ± 0.12	0.86	86.2%	5.97 ± 0.14	325.5 ± 15	8	0.94	6.28 ± 0.14	Duplicate of above
55010	MI91-C27a	Martha	6.19 ± 0.05	1.20	99.3%	6.15 ± 0.05	297.3 ± 2.6	8	1.35	6.26 ± 0.08	Coarse adularia crystals in host rock

TABLE 1. (*Cont.*)

AU no.	CM Hall no.	Location	Plateau	MSWD	F39 (%)	Isochron	40/36 Intercept	n	MSWD	Total gas	Comments
55010	MI91-G27b	Martha	5.96 ± 0.05	0.67	69.0%					6.13 ± 0.09	Duplicate of above
59723	MC24-m4a	Muirs Reef	2.12 ± 0.11	1.6	93.5%					2.38 ± 0.22	Adularia from quartz vein
59723	MC24-m4b	Muirs Reef	1.78 ± 0.16	1.53	96.1%					2.30 ± 0.26	Duplicate of above
59723	MC24-m4c	Muirs Reef	n/a							2.15 ± 0.12	Duplicate of above
59719	MC24-m5a	Ohui	8.25 ± 0.55	1.93	95.9%					8.18 ± 0.62	Adularia from quartz vein
59719	MC24-m5a	Ohui				8.31 ± 0.20	-6.2 ± 86	7	0.06		Plateau points
59719	MC24-m5b	Ohui	8.42 ± 0.50	0.94	80%	8.53 ± 1.18	599.2 ± 1731	13	1.27	8.88 ± 0.79	Duplicate of above
59719	MC24-m5b	Ohui				8.47 ± 0.27	43.7 ± 143	5	0.13		Plateau points
59719	MC24-m5c	Ohui	8.24 ± 0.35	0.17	92.2%	8.24 ± 0.34	277.5 ± 126	13	0.62	8.35 ± 0.49	Duplicate of above
59719	MC24-m5c	Ohui				8.52 ± 2.29	-558.0 ± 6654	6	0.11		Plateau points
56760	MC07-S22a	Opitonui	13.17 ± 0.07	0.65	97.6%	13.25 ± 0.07	286.8 ± 3.2	13	0.65	13.02 ± 0.10	Adularia from quartz vein
56760	MC07-S22a	Opitonui			76%	13.24 ± 0.12	287.3 ± 11	10	0.46		Plateau points
56760	MC07-S22b	Opitonui	13.14 ± 0.08	0.67						12.96 ± 0.09	Duplicate of above
56760	MC07-S22b	Opitonui				13.01 ± 0.96	320.5 ± 180	4	0.96		Plateau points
56761	MC07-S23a	Opitonui	13.12 ± 0.07	0.48	100%	13.13 ± 0.07	292.9 ± 4.4	13	0.39	13.09 ± 0.10	Adularia from quartz vein
56761	MC07-S23a	Opitonui				13.01 ± 0.96	320.5 ± 180	4	0.96		Plateau points
56761	MC07-S23b	Opitonui	13.20 ± 0.11	1.77	97.9%		274.8 ± 24.4			13.10 ± 0.07	Duplicate of above
56761	MC07-S23b	Opitonui									Plateau points
56762	MC07-S24a	Opitonui	12.82 ± 0.09	1.21	98.1%	12.82 ± 0.10	295.5 ± 4.8	13	1.61	12.77 ± 0.12	Duplicate of above
56762	MC07-S24a	Opitonui				12.84 ± 0.09	289.4 ± 5.4	11	0.82		Plateau points
56762	MC07-S24b	Opitonui	13.14 ± 0.08	1.26	86.2%	13.15 ± 0.09	286.7 ± 2.6	13	1.53	12.79 ± 0.11	Adularia from quartz vein
56762	MC07-S24b	Opitonui				13.21 ± 0.14	261.0 ± 59	8	1.24		Plateau points
56763	MC07-S25a	Paritu	16.32 ± 0.13	1.69	55.3%	16.51 ± 0.31	284.0 ± 17	5	1.41	16.19 ± 0.13	Adularia from quartz vein
56763	MC07-S25a	Paritu	-								Plateau points
56763	MC07-S25b	Paritu								16.36 ± 0.21	Duplicate of above
56758	MC07-S20a	Sovereign	6.81 ± 0.06	0.98	96.4%	6.70 ± 0.07	297.4 ± 0.6	13	1.07	7.06 ± 0.11	Host-rock adularia
56758	MC07-S20a	Sovereign				6.87 ± 0.20	294.4 ± 3.4	10	1.05		Plateau points
56758	MC07-S20b	Sovereign	-							6.87 ± 0.15	Duplicate of above
56759	MC07-S21a	Sovereign	6.56 ± 0.08	0.93	62.1%					6.30 ± 0.11	Host-rock adularia
56759	MC07-S21a	Sovereign				6.57 ± 0.09	295.4 ± 1.4	7	1.12		Plateau points
56759	MC07-S21b	Sovereign	6.55 ± 0.04	0.68	68.6%	6.53 ± 0.06	298.8 ± 7.2	7	0.65	6.47 ± 0.04	Duplicate of above
56759	MC07-S21b	Sovereign				6.69 ± 0.18	297.4 ± 12	13	0.89		Plateau points
59721	MC24-m7a	Sovereign	6.69 ± 0.17	0.82	100%					6.70 ± 0.32	Adularia from quartz vein
59721	MC24-m7b	Sovereign	6.74 ± 0.38	0.71	94.4%					6.58 ± 1.02	Duplicate of above
59721	MC24-m7b	Sovereign				6.97 ± 0.50	214.8 ± 149	3	0.72		Plateau points
59721	MC24-m7c	Sovereign	n/a							6.37 ± 0.19	Duplicate of above
33870	MC07-S18a	Waiorongomai	5.74 ± 0.04	0.81	99.3%	5.75 ± 0.04	292.5 ± 3.8	11	0.62	5.82 ± 0.06	Coarse adularia in quartz vein
33870	MC07-S18a	Waiorongomai									Plateau points
33870	MC07-S18b	Waiorongomai	5.68 ± 0.04	1.44	99.5%	5.68 ± 0.04	296.8 ± 2.2	13	1.53	5.74 ± 0.06	Duplicate of above
33870	MC07-S18b	Waiorongomai				5.68 ± 0.04	295.4 ± 4.2	12	1.59		Plateau points
33973	MC07-S19a	Waiorongomai	5.72 ± 0.09	0.96	89.0%	5.75 ± 0.10	281.8 ± 5.8	13	1.32	5.56 ± 0.14	Adularia bands in quartz-base metal sulfide vein
33973	MC07-S19a	Waiorongomai				5.65 ± 0.16	320.9 ± 42	10	0.87		Plateau points
33973	MC07-S19b	Waiorongomai	5.74 ± 0.07	1.06	100%	5.77 ± 0.07	287.7 ± 9.2	13	0.90	5.67 ± 0.10	Duplicate of above
56755	MC07-S29a	Wharekirauponga	6.24 ± 0.08	0.54	100%	6.24 ± 0.10	295.5 ± 4.4	13	0.59	6.26 ± 0.13	Adularia from colloform quartz vein
56755	MC07-S29b	Wharekirauponga	6.37 ± 0.07	1.16	98.3%	6.38 ± 0.07	293.3 ± 3.4	13	1.33	6.33 ± 0.07	Duplicate of above
56755	MC07-S29b	Wharekirauponga				6.32 ± 0.18	305.4 ± 31	11	1.24		Plateau points

For the Re-Os dates of samples from Ohio Creek and Martha, we used the methods of Barra et al. (2003), and the analytical work was undertaken at the University of Arizona. Approximately 0.02 to 0.1 g of pure molybdenite was hand-picked and loaded into a Carius tube. Spikes of [185]Re and [190]Os were added, along with 8 mL of reverse aqua regia (three parts of HNO_3, 16 N, and one part of HCl, 10 N). About 2 to 3 mL of hydrogen peroxide (30%) was added to ensure complete oxidation of the sample and spike equilibration. The tube was heated to 240°C for approximately 8 h, and the solution was later subjected to a two-stage distillation process for osmium separation (Nägler and Frei, 1997). Osmium was later purified using a microdistillation technique described by Birck et al. (1997) and loaded on platinum filaments with $Ba(OH)_2$ to enhance ionization. After osmium separation, the remaining acid solution was dried, and the residue was dissolved in 0.1 N HNO_3. Rhenium was extracted and purified through a two-stage column using AG1-X8 (100–200 mesh) resin and loaded on nickel filaments with $BaNO_3$.

Samples were analyzed by negative thermal ion mass spectrometry using methods discussed in Barra et al. (2003). Uncertainties were calculated using error propagation, taking into consideration errors from spike calibration, the uncertainty in the rhenium decay constant (0.31%), and analytical errors. All rhenium and osmium in molybdenite samples were measured with Faraday collectors. Blank corrections were insignificant for natural Os. In some cases, replicate analyses of single molybdenite samples were performed; in other cases, samples were analyzed only once because the date obtained was identical to other samples of the same deposit or the amount of sample was limited.

Results

Table 1 shows [40]Ar/[39]Ar dates of adularia from the Paritu, Opitonui, Ohui, Broken Hills, Wharekirauponga, Maratoto, Sovereign, Jubilee/Scotia, Karangahake, Martha, Favona, Waiorongomai, Eliza, and Muirs Reef deposits (App. 2). Errors within the samples are 2σ, and all samples fall beneath

the mean MSWD of 2. The samples were run twice, and Table 1 also shows the duplicate analyses.

Table 2 shows preferred ages for orebodies of the Hauraki goldfield, and the basis for their determinations. In this manuscript, we use accepted nomenclature where "date" refers to the date derived from a single determination, and "age" is the actual time when the deposit formed, which may be a single date or an average of several dates (cf. Richards and Noble, 1998).

Adularia from a tourmaline-bearing quartz vein at Paritu yields a single [40]Ar/[39]Ar plateau date of 16.32 ± 0.13 Ma (2σ) from steps 9 through 13 (55% of gas), and total gas dates of 16.19 ± 0.13 and 16.36 ± 0.21 Ma (Table 1; Fig. 5A). Steps 9 through 13 define an isochron with a date of 16.51 ± 0.31 Ma, an MSWD of 1.41, with no indication of excess argon, and overlaps within error of the plateau date. Thus, we use the plateau date as the preferred age of this sample (Table 2). Previous K-Ar results for the Paritu diorite pluton provided dates of 16.0 to 17.1 Ma (Richards et al., 1966). When readjusted using Steiger and Jäger (1977) decay constants, these dates range from 16.4 to 17.6 Ma (Adams et al., 1994). This range, combined with the single date from our work, is consistent with mineralization occurring soon after emplacement of the pluton, but additional geochronology on the plutonic rocks and veins has great potential to provide much tighter constraints on the timing of plutonic activity, mineralization, and uplift in this area.

Three samples of adularia from quartz veins from Opitonui yield six [40]Ar/[39]Ar plateau dates that range from 12.82 ± 0.09 to 13.17 ± 0.07 Ma. Five plateaus give exceptionally flat spectra that overlap within error, although one replicate plateau yielded a slightly younger date, presumably due to minor Ar loss. An error weighted average of the five plateaus that overlap is $13.15 \pm .03$ Ma, and the MSWD of the average is 0.25; we use this as the preferred age of the deposit (Tables 1, 2; Fig. 5B). The samples yielded nine isochrons with MSWD values less than 2.0, and seven of these yield dates that overlap with the five plateau dates above, and three of the six total

TABLE 2. Summary of Preferred Ages for the Hauraki Goldfield

| Location	Province	Preferred age (Ma)	Comments	Reference
Broken Hills	Eastern	7.12 ± 0.02	Average of four [40]Ar/[39]Ar plateaus from adularia from two quartz veins	This study
Eliza	Southern	4.47 ± 0.06	Average of two [40]Ar/[39]Ar plateaus from adularia from one quartz vein	This study
Favona	Southern	6.05 ± 0.08	Average of two [40]Ar/[39]Ar plateaus from adularia from one quartz vein	This study
Golden Cross	Southern	6.98 ± 0.11	Average of four [40]Ar/[39]Ar plateaus from adularia from two quartz veins	Mauk and Hall (2004)
Karangahake	Southern	6.9 to 6.1	Three [40]Ar/[39]Ar dates of adularia from two quartz veins	This study
Komata	Southern	6.06 ± 0.06	Average of two [40]Ar/[39]Ar plateaus from coarse adularia from one vein	Mauk and Hall (2004)
Kuaotunu	Northern	14.1 ± 0.2	K-Ar adularia	Skinner (1986)
Maratoto	Southern	6.41 ± 0.04	Average of four [40]Ar/[39]Ar plateaus from adularia from three quartz veins	This study
Martha	Southern	6.16 ± 0.06	Average of two [40]Ar/[39]Ar plateaus from adularia from one quartz vein	This study
Muirs Reef	Southern	2.1 to 1.8	[40]Ar/[39]Ar plateau dates of adularia from one quartz vein	This study
Neavesville	Eastern	6.88 ± 0.04	Average of four [40]Ar/[39]Ar plateaus from coarse adularia from two veins	Mauk and Hall (2004)
Ohio Creek	Northern	12.0 to 11.9	Re-Os molybdenite	This study
Ohui	Eastern	8.29 ± 0.25	Average of three [40]Ar/[39]Ar plateaus from adularia from one quartz vein	This study
Opitonui	Northern	13.15 ± .03	Average of five [40]Ar/[39]Ar plateaus from adularia from three quartz veins	This study
Paritu	Northern	16.32 ± 0.13	Single [40]Ar/[39]Ar plateau date of adularia from one quartz vein	This study
Sovereign	Southern	6.70 ± 0.16	Average of two [40]Ar/[39]Ar plateaus from adularia from one quartz vein	This study
Waiorongomai	Southern	5.71 ± 0.03	Average of four [40]Ar/[39]Ar plateaus from adularia from two veins	This study
Waiomu	Northern	10.8 ± 0.1	K-Ar sericite	Skinner (1986)
Wharekirauponga	Eastern	~6.3	Average of two [40]Ar/[39]Ar plateaus from adularia from one quartz vein	This study

Note: all averages listed above are error weighted
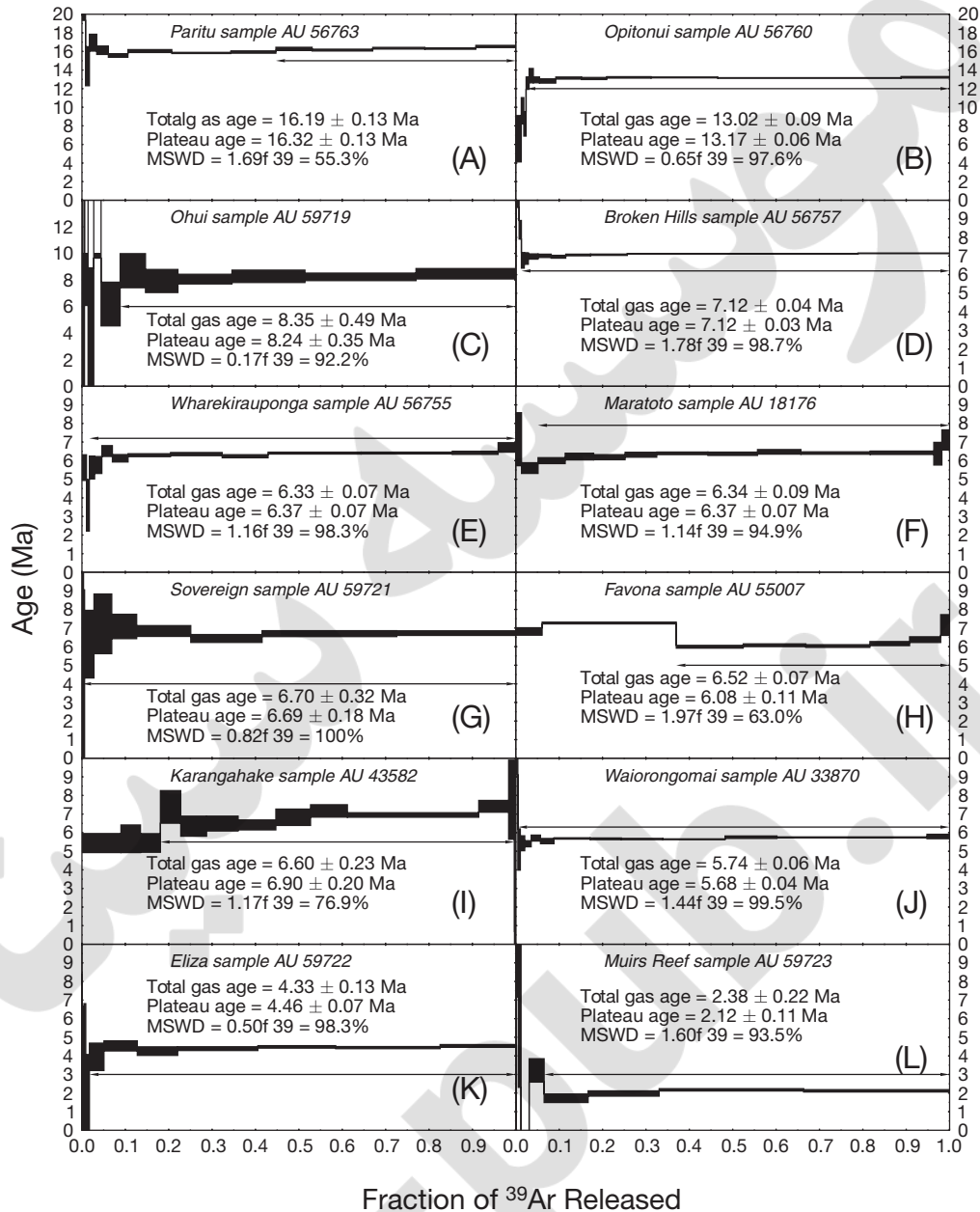
FIG. 5. Representative age spectra for samples of adularia from quartz veins. All error estimates are 2σ and error boxes are 1σ. The double arrows show the extent of the plateaus and the steps included in the plateaus, and f39 is the fraction of ^{39}Ar that was released. A. Paritu sample AU 56763 (MC07-S25a). B. Opitonui sample AU 56760 (MC07-S22a). C. Ohui sample AU 59719 (MC24-m5c). D. Broken Hills sample AU 56757 (MC07-S17a). E. Wharekirauponga sample AU 56755 (MC07-S29b). F. Maratoto sample AU 18176. (MC07-S15a). G. Sovereign sample AU 59721 (MC24-m7a). H. Favona sample AU 55007. (MI91-G26b). I. Karangahake sample AU 43582. (MC07-S27a). J. Waiorongomai sample AU 33870. (MC07-S18b). K. Eliza sample AU 59722 (MC24-m3b). L. Muirs Reef sample AU 59723 (MC24-m4a).

gas dates also overlap with these plateau dates (Table 1). One plateau, two isochrons, and three total gas dates cluster around 12.8 Ma and overlap within error, but we prefer the older age of 13.15 ± 0.03 Ma because the plateaus used to derive that age are exceptionally flat and very reproducible (Fig. 5B). Host rocks from the Kuaotunu Subgroup have whole-rock K-Ar dates of 11.4 Ma, and unaltered plagioclase from the Mahinapua Andesite yielded a date of 13.8 ± 0.3 Ma (Skinner, 1986). Given the 13.15 Ma age of mineralization at Opitonui

and the 13.8 Ma date for the plagioclase separate, it is likely that the 11.4 Ma whole-rock date is too young.

One sample of molybdenite from 337.9-m depth in DDH 6 at Ohio Creek yielded total Re and ^{187}Os concentrations of 1,191 to 1,334 ppm and 149 to 165 ppb, respectively (Table 2). The two Re-Os dates overlap within error and yield dates of 11.87 ± 0.06 and 11.97 ± 0.08 Ma (2σ). These samples are slightly older than the K-Ar date of 11.2 ± 0.3 Ma determined on hypogene alunite from altered rocks of the advanced

argillic cap at Ohio Creek (Hunt and Roddick, 1992) and significantly older than the $^{40}Ar/^{39}Ar$ date of 10.71 ± 1.35 Ma of a relatively unaltered hornblende-augitie dacitic porphyry dike (Hunt and Roddick, 1993). Both molybdenite samples have high Re and ^{187}Os concentrations and overlap within error. The discrepancy between the hypogene alunite and molybdenite dates may be explained by (1) slightly protracted or episodic mineralization, (2) Re and Os has a higher closure temperature in molybdenite than K-Ar in alunite, so the former method may yield the age of mineralization whereas the latter might yield the cooling age, or (3) that the K-Ar date is slightly disturbed. Based on the comparative studies of K-Ar and $^{40}Ar/^{39}Ar$ dates presented in this paper, we prefer (3), but the other two possibilities cannot be ruled out.

Hydrothermal mineralization at Thames is constrained by K-Ar dates of 11.6 ± 0.3 to 10.9 ± 0.2 Ma from illite selvages of auriferous quartz veins in the eastern part of the Thames district (Sinsuat, 1992). However, the K-Ar dates of the illite are particularly subject to analytical uncertainties, and therefore we interpret the likely age of mineralization at Thames as between 12 and 11 Ma. Within this interval, it is likely closer to 12 Ma, based on our new Re-Os results and also on the geologic data that suggests a genetic relationship between the Ohio Creek and Thames mineralization (e.g., Brathwaite et al., 2001b).

One sample of adularia from a quartz vein at the Phoenix workings in the Ohui deposit yielded three $^{40}Ar/^{39}Ar$ plateau dates that overlap within error and range from 8.24 ± 0.35 to 8.42 ± 0.50 Ma. An error weighted average of the three plateaus that overlap is 8.29 ± 0.25 Ma, and the MSWD of the average is 0.19; we use this as the preferred age of the deposit (Tables 1, 2; Fig. 5C). The samples yielded six isochrons with MSWD values less than 2.0 and three total gas dates that overlap with the plateau dates, although three of the isochrons have 2σ errors that exceed 1 Ma (Table 1). Mineralization occurs in both Coromandel Group andesite and Whitianga Group rhyolite, but the absolute ages of the host rocks at Ohui are not well-constrained, and therefore the timing between mineralization and volcanism remains unclear.

Two samples of rhombohedral adularia crystals from the Night Reef at the Broken Hills deposit yield four exceptionally flat $^{40}Ar/^{39}Ar$ plateaus that range from 7.12 ± 0.03 to 7.15 ± 0.05 Ma (Table 1; Fig. 5D). These results overlap within error to give an average of 7.12 ± 0.02 Ma, which is our preferred age of the deposit; the MSWD of the average is 0.46 (Table 2). The samples yielded four isochrons with MSWD values less than 2.0 and four total gas dates, all of which overlap with the plateau dates and our preferred age (Table 1). Obsidian from the Whitianga Group host rocks has fission track and K-Ar dates that indicate that volcanism in the region occurred between 7.2 and 7.8 Ma (Skinner, 1986) and suggest that Broken Hills mineralization occurred shortly after rhyolite volcanism.

Adularia from one sample of a colloform quartz vein in the Wharekirauponga prospect yields $^{40}Ar/^{39}Ar$ plateaus of 6.24 ± 0.08 and 6.37 ± 0.07 (Table 1; Fig. 5E). The dates overlap within error to give an average of 6.32 ± 0.12 Ma, but the MSWD of the average is 5.51, and the combined age fails the chi-squared statistical test of Wendt and Carl (1991), so our

preferred age of the Wharekirauponga prospect is approximately 6.3 Ma (Table 2). The sample also yielded three isochrons with MSWD values less than 2.0 and four total gas dates, all of which overlap with the plateau dates and our preferred age (Table 1). Veins at the Wharekirauponga prospect occur in the Maratoto Rhyolite, which elsewhere in the region has K-Ar dates between 7 to 6 Ma (Brathwaite and Christie, 1996). Postmineralization Whakamoehau Andesite near the prospect has a K-Ar date of 6.61 ± 0.12 Ma (Brathwaite and Christie, 1996), which is older than our preferred age of mineralization. Therefore, more work is required to refine the relationships between volcanism and mineralization in the Wharekirauponga area.

Six $^{40}Ar/^{39}Ar$ plateau dates of three adularia samples from quartz veins at the Maratoto deposit range from 6.29 ± 0.08 to 6.60 ± 0.07 Ma (Table 1; Fig. 5F). Four of these values overlap within error, and the average of these values is 6.41 ± 0.04 Ma, which we interpret as the preferred age for the deposit; the MSWD of the average is 1.44 (Table 2). The sample also yielded eight isochrons with MSWD values less than 2.0 that overlap with the above plateau dates and our preferred age, and four total gas dates also overlap with these results (Table 1). One plateau and two isochrons yield dates of approximately 6.6 Ma, which are older than our preferred age of 6.41 Ma. Although this may indicate protracted mineralization, this seems unlikely for this sample, which is a duplicate analysis of a single clot of coarse-grained adularia in a coarse-grained quartz vein. Because we were not analyzing adularia from different bands within the vein, or different vein samples, this discrepancy is difficult to explain. Nonetheless, our preferred age of 6.4 Ma is similar to previous K-Ar dates of adularia from veins of 6.2 ± 0.1 to 5.2 ± 0.1 Ma (Skinner, 1986), and our results suggest that the deposit formed at the waning stages of deposition of the host 7.9 to 6.3 Ma Waipupu Formation (Brathwaite and Christie, 1996).

One sample of adularia from a quartz vein at the Sovereign deposit yielded $^{40}Ar/^{39}Ar$ plateau, isochron, and total gas dates of approximately 6.7 Ma. All dates overlap within error, and these dates also overlap the plateau, isochron, and total gas dates of host-rock adularia from the Sovereign deposit (Table 1; Fig. 5G). We therefore used the average of the two vein adularia plateau dates, which is 6.70 ± 0.16 Ma with an MSWD of 0.07, as the preferred age for the Sovereign deposit (Table 2). The Sovereign deposit is hosted by the 7.9 to 6.3 Ma Waipupu Formation (Brathwaite and Christie, 1996), but uncertainties in the absolute ages of the host rocks at Sovereign preclude any rigorous interpretations of the relationship between volcanism and mineralization.

A small quartz-adularia vein near the Sovereign deposit, in the area between the Jubilee and Scotia deposits, yielded plateau, isochron, and total gas dates that overlap within error (AU 59720; Table 1). The plateau dates barely overlap at the 2σ level to yield an average of 6.19 ± 0.12 Ma, but the MSWD is 6.35, and the combined age fails the chi-squared statistical test of Wendt and Carl (1991), so we interpret the age of this vein as approximately 6.2 Ma. This age does not overlap with our preferred age of the Sovereign deposit, and therefore, we interpret this vein as representing fracture-controlled fluid flow adjacent to the Sovereign deposit at a later time.

Three samples of adularia from host rocks at the Martha deposit yielded five $^{40}Ar/^{39}Ar$ plateau dates that range from 5.96 ± 0.05 to 6.19 ± 0.05 Ma, and a grab sample of adularia from a quartz vein at Martha yielded two $^{40}Ar/^{39}Ar$ plateau dates of 6.14 ± 0.04 and 6.20 ± 0.07 (Table 1; Fig. 6). We consider the dates from the adularia within the quartz vein to be the most robust, because adularia from host rocks commonly shows some replacement by illite, whereas adularia from veins is unaltered. The alteration of host-rock adularia likely contributes to the larger errors and more irregular spectra obtained from host-rock adularia (Fig. 6A); in contrast spectra from vein adularia are relatively flat and have significantly smaller errors (Fig. 6B). The two dates from vein adularia at Martha overlap within error, produce an error weighted mean total gas date of 6.19 ± 0.05 Ma, an error weighted mean plateau date of 6.16 ± 0.06 Ma, and an error weighted isochron date of 6.12 ± 0.06 Ma. All three dates overlap within error, and we use the average of the plateau dates to interpret a preferred age for this vein sample of 6.16 ± 0.06 Ma; we also use this as the preferred age of the Martha deposit (Table 2).

Samples of molybdenite from two other veins in the deep levels of the Martha deposit have total Re and ^{187}Os concentrations of 136 and 299 ppm and 9.0 and 20 ppb, respectively, and Re-Os dates of 6.37 ± 0.03 and 6.51 ± 0.03 Ma. These dates do not overlap with each other, and we interpret each date to be the age of each molybdenite-bearing vein (Table 3). The $^{40}Ar/^{39}Ar$ plateau dates of vein adularia and the Re-Os molybdenite dates are similar to a previously reported K-Ar date of 6.58 ± 0.54 Ma, but significantly younger than other

K-Ar dates of 6.92 ± 0.30 and 7.23 ± 0.38 Ma determined on adularia from strongly altered andesite at the Martha deposit (Brathwaite and Christie, 1996). These K-Ar dates overlap with or exceed the 6.12 to 6.43 Ma total gas dates of adularia in this study (Table 1), which are equivalent to K-Ar dates. These older dates may reflect excess argon in these hydrothermal samples, which may occur in fluid inclusions in the adularia or other minerals that were included in the samples. Results from our step-heated spectra support this, because they commonly show older ages and a spike in the Cl/K values at the beginning of the run, indicating that there is a relatively large release of Cl at the beginning of the run (Fig. 6). The Cl likely comes from the abundant fluid inclusions in these samples.

Adularia from one quartz vein from the Moonlight portion of the Favona deposit yields $^{40}Ar/^{39}Ar$ plateaus of 6.01 ± 0.14 and 6.07 ± 0.10 Ma (Table 1; Fig. 5H). The dates overlap within error giving our preferred age for the Favona deposit of 6.05 ± 0.08 Ma. This preferred age for the Favona deposit overlaps within error with our preferred age of 6.16 ± 0.06 Ma for the Martha deposit, indicating that these deposits formed more or less synchronously at 6.1 Ma. This supports previous interpretations that both deposits formed within the same hydrothermal system, as indicated by geologic, fluid inclusion, mineralogical, and geophysical constraints (e.g., Brathwaite and Faure, 2002; Simpson and Mauk, 2007; Morrell et al., 2011).

Host-rock adularia from the Karangahake deposit yields $^{40}Ar/^{39}Ar$ plateau dates of 5.71 ± 0.13 and 5.75 ± 0.10 Ma (Table 1; Fig. 5I). Two samples of adularia from different
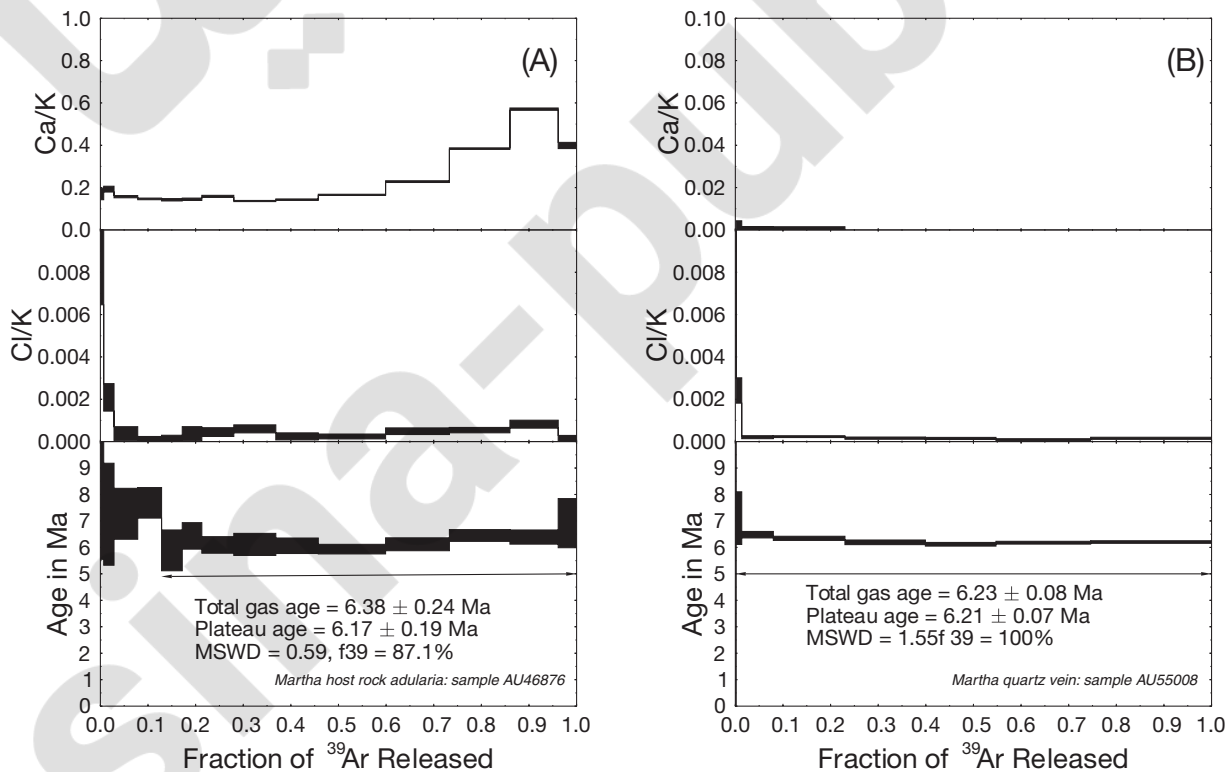

FIG. 6. Age spectra from two adularia samples from the Martha deposit. All error estimates are 2σ and error boxes are 1σ. A. Host-rock adularia from sample AU46876 (MI91-G19a). B. Adularia from quartz vein sample AU55008 (MI91-G20c).

TABLE 3. Re-Os Data for Molybdenite from the Ohio Creek and Waihi Deposits (all errors are ±2σ)

AU no.	Northing	Easting	Location	Comments	Weight (g)	Total Re (ppm)	^{187}Re (ppm)	^{187}Os (ppb)	Age (Ma)	Error (2σ)
59724	6420700	2762700	Waihi	Waihi extension: 1916: molybdenite veins from deep levels of the Waihi deposit	0.113	135.6	84.9	9.01	6.37	0.03
59725	6420700	2762700	Waihi	Molybdenite from the deep levels of the Waihi deposit	0.021	298.5	186.9	20.3	6.51	0.03
59726	6452400	2737200	Ohio Creek	DDH 6- 337.9 m; molybdenite from porphyry depost near Thames	0.067	1333.9	835.0	165.2	11.87	0.06
59726			Ohio Creek	DDH 6- 337.9 m; molybdenite from porphyry depost near Thames	0.055	1190.7	745.4	148.6	11.97	0.08

quartz veins in the deposit yield three ^{40}Ar/^{39}Ar plateau dates ranging from 6.12 ± 0.23 to 6.90 ± 0.20 Ma (Table 1; Fig. 5I). Although the dates from the host-rock adularia overlap within error, petrographic analysis shows that late illite replaces this host-rock adularia, and therefore these plateau dates are likely disturbed. Dates from the quartz vein adularia do not overlap, and the host-rock adularia dates are up to 1.2 Ma younger than the dates of adularia from the veins. Therefore, we cannot interpret a single preferred age for mineralization at Karangahake. Previous K-Ar results from Karangahake also reflect this complexity. Adularia from altered andesite and associated mineralization at Karangahake yielded K-Ar dates of 4.8 ± 0.1 and 6.0 ± 0.1 Ma (Skinner, 1986). The 6 to 7 Ma Maratoto Rhyolite of the Whitianga Group forms a cap over 7.9 to 6.3 Ma Waipupu Formation andesite at Mount Karangahake (Brathwaite, 1989; Brathwaite and Christie, 1996). Stockwork quartz veins cut the rhyolite cap, so some of the mineralization must be younger than the Maratoto Rhyolite. We recognize three possible explanations for these complex and apparently conflicting results: (1) the Karangahake area may have undergone more than one phase of mineralization, (2) hydrothermal alteration of the host rocks may have continued for a long period of time after the veins we dated had formed, or (3) the Karangahake deposit formed at relatively deep levels at higher temperatures than most deposits in the Hauraki goldfield (Brathwaite, 1989; Christie et al., 2007), and therefore some of the dates may be cooling ages rather than crystallization ages. Of these, we consider (1) and (2) to be most likely, but (3) cannot be ruled out.

Adularia from the Waiorongomai deposit was extracted from a quartz vein and from a quartz-base metal sulfide vein, and yielded ^{40}Ar/^{39}Ar plateaus that range from 5.68 ± 0.04 to 5.74 ± 0.04 Ma (Fig. 5J). The results overlap within error (Table 1), and the average of the four plateaus is 5.71 ± 0.03 Ma, which we use as our preferred age of mineralization at the Waiorongomai deposit; the MSWD of the average is 1.95 (Table 2). The samples also yielded six isochrons with MSWD values less than 2.0 that overlap with our preferred age, and three of the four total gas dates also overlap with the plateau dates and our preferred age (Table 1). Andesitic volcanic rocks have yielded K-Ar dates of 6.65 Ma from an area near the Waiorongomai deposit, which is consistent with the age of the Waipupu Andesite (Brathwaite and Christie, 1996).

One sample of adularia from a quartz vein at the Eliza deposit yielded two ^{40}Ar/^{39}Ar plateau dates of 4.49 ± 0.12 and 4.46 ± 0.07 Ma, which overlap within error. An error weighted average of these plateaus is 4.47 ± 0.06 Ma, which is our preferred age of the Eliza deposit, and the MSWD of this average is 0.12 (Table 1; Fig. 5K). The samples yielded four isochrons with MSWD values less than 2.0 and two total gas dates that overlap with the plateau dates (Table 1).

One sample of adularia from a quartz vein at the Muirs Reef deposit yielded two ^{40}Ar/^{39}Ar plateau dates and three total gas dates that range from 1.78 to 2.38 Ma (Table 1; Fig. 5L). The older plateau date overlaps the three total gas dates within error, but the younger plateau date does not overlap the other dates. Therefore, rather than interpreting a single preferred age for the Muirs Reef deposit, we conclude that it formed between 2.1 and 1.8 Ma (Table 2).

Discussion

Epithermal and porphyry deposits in the Hauraki goldfield show ages that progressively young southward and cluster into two groups that are distinct in time (Fig. 7). The northern province of the goldfield contains deposits that are older than 11 Ma, and the southern and eastern provinces contain deposits that are younger than 8.3 Ma (Mauk and Hall, 2004; Ward et al., 2005; Christie et al., 2007). Deposits in different provinces show some significant differences, and there is also a change in volcanic activity, and more speculatively, structural style that coincides with the 11 to 8.3 Ma hiatus between deposits in the northern versus those in the southern and eastern provinces. This section begins with a discussion of the possible duration of hydrothermal mineralization in the Waihi district and the implications of our data for metallogeny. We then synthesize available data about mineralization, volcanism, and structural setting of the deposits and conclude by evaluating hypotheses for the tectonic and volcanologic evolution of the Hauraki goldfield and its links with epithermal mineralization.

Duration of hydrothermal mineralization in the Waihi district

The Waihi district contains both the Martha mine and the recently discovered Favona deposit (Brathwaite et al., 2006; Mauk et al., 2006b, Torckler et al., 2006; Simpson and Mauk, 2007). Both deposits sit within a single magnetic quiet zone
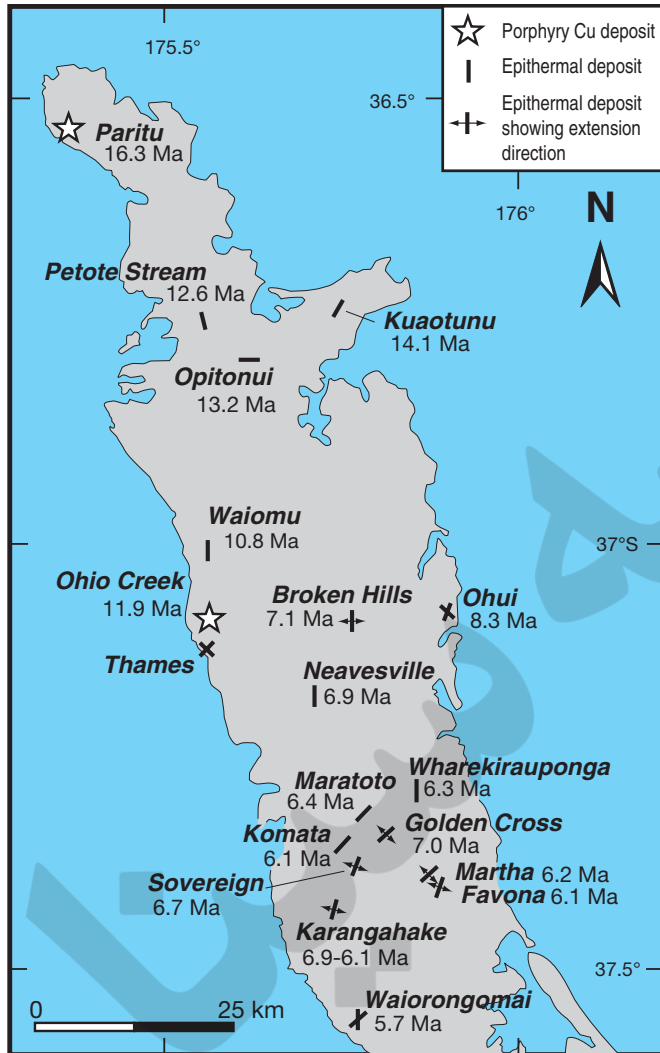
FIG. 7. Map of the Hauraki goldfield, showing the ages of epithermal and porphyry deposits, and also the direction of extension, where constrained from kinematic indicators. Data sources in text.

required to establish whether the molybdenite veins, which are very rare, formed from the same type of hydrothermal system as the epithermal orebodies at Martha and Favona, or whether they formed from a different type of earlier hydrothermal activity. Nonetheless, the overall longevity of hydrothermal activity in the Waihi district is clearly indicated by our dates.

Elsewhere, constraints on the lifespans of the hydrothermal systems that formed epithermal deposits are relatively uncommon. Some of these suggest that mineralization occurred during a long time interval, whereas others provide evidence for mineralization forming during a brief time window. For example, the Hosen vein at Hishikari, Japan, formed during a period of 260,000 years, and the hydrothermal system that produced the mineralization had a lifetime of approximately 600,000 years, lasting between 1.25 and 0.64 Ma (Sanematsu et al., 2006, and references therein). There is still geothermal activity at Hishikari, which suggests that the hydrothermal system may have been active, in some form, for 1.25 Ma. The Ladolam gold deposit on Lihir Island, Papua New Guinea, formed approximately 0.6 to 0.5 Ma (Carman, 2003). The area remains an intense center of geothermal activity, with a variety of geothermal manifestations in the open pit and an estimated heat flow of 50 to 70 mW (Simmons and Brown, 2006). In contrast, Henry et al. (1997) provided $^{40}Ar/^{39}Ar$ geochronology from the Round Mountain deposit in Nevada, which indicates that this 16 Moz orebody may have formed in as little as 0.05 Ma. Similarly, Leavitt et al. (2004) obtained dates from several veins at Midas in Nevada, and all dates essentially overlapped within error, indicating that this deposit also formed in a short time period.

Future work in the Hauraki goldfield and elsewhere should endeavor to address two important questions: what is the total duration of hydrothermal activity that leads to epithermal orebodies, and does mineralization in individual deposits form from discrete, episodic events that are separated by significant time lags or does mineralization form more or less continuously through time? We note, for example, that most vein textures suggest the former, whereas most geochemical models assume the latter.

Progression of ages, metallogenic trends, and
Au deposition through time

The geochronology of mineral deposits in the northern Hauraki goldfield remains incomplete, in part because of local absence of suitable material such as vein adularia or molybdenite for dating. Nonetheless, the available data clearly show southward-younging of mineralization, which ranges from 16.3 Ma in the north to 12 Ma in the south near Thames (Fig. 2; Table 3). The oldest mineralization is in the northern part of the goldfield at Paritu, which is constrained by our single $^{40}Ar/^{39}Ar$ plateau date of 16.3 Ma. Adularia from the Kuaotunu deposit yielded a K-Ar date of 14.1 ± 0.2 Ma (Skinner, 1986), which is significantly older than our preferred age of 13.1 Ma for adularia from the nearby Opitonui deposit. Sericite from Waiomu has a K-Ar date of 10.8 ± 0.1 Ma (Skinner, 1986), and our results lead us to prefer a 12 Ma age for mineralization at Ohio Creek and Thames.

There is a temporal and spatial hiatus of mineralization between the northern province and the southern and eastern provinces of the Hauraki goldfield, even though volcanic

that was produced by destruction of magnetite in the host volcanic rocks during hydrothermal alteration (Morrell et al., 2011). Previous workers agree that geological and geophysical evidence is consistent with both deposits forming from the same hydrothermal system (e.g., Brathwaite and Faure, 2002; Torckler et al., 2006; Simpson and Mauk, 2007; Morrell et al., 2011). Our preferred ages of the Martha and Favona deposits overlap within error (6.16 ± 0.06 and 6.05 ± 0.08 Ma, respectively) and support this hypothesis.

The Re-Os dates of 6.37 ± 0.03 and 6.51 ± 0.03 Ma of molybdenite-bearing veins from deeper levels of the Martha deposit do not overlap within error and are older than our preferred $^{40}Ar/^{39}Ar$ age of vein adularia from shallower levels of the deposit. Therefore, available data indicate that hydrothermal systems were active in the Waihi district from 6.5 to 6.1 Ma, with a span of approximately 390,000 to 460,000 years. However it is also possible that the molybdenite and gold veins are the product of shorter lived but separate hydrothermal systems that overlap spatially. Additional work is

activity during this period appears to be more continuous (Fig. 2; Table 3). The data suite from the southern and eastern goldfield is more robust, with the oldest ages from the Ohui (8.3 Ma), Broken Hills (7.1 Ma), Neavesville (6.9 Ma), Golden Cross (6.9 Ma), and Sovereign (6.7 Ma) deposits. Mineralization continued at Maratoto (6.4 Ma), Wharekirauponga (6.3 Ma), Komata (6.1 Ma), Martha and Favona (6.1 to 6.0 Ma), and then at the Waiorongomai (5.7 Ma), Eliza (4.5 Ma), and Muirs Reef (2.1 to 1.8 Ma) deposits (Mauk and Hall, 2004; this paper).

In general, the ages of mineralization young from north to south, but some important variations exist. For example, unaltered volcanic rocks in the Hauraki goldfield typically show short-wavelength high-amplitude magnetic anomalies but areas underlain by altered volcanic rocks whose magnetite has been destroyed by hydrothermal alteration show magnetic quiet zones (Locke et al., 2006; Morrell et al., 2011). A single large magnetic quiet zone in the southern goldfield envelops the Maratoto (6.4 Ma), Golden Cross (6.9 Ma), Komata (6.1 Ma), and Sovereign (6.7 Ma) deposits (Morrell et al., 2011). However, the variable ages of these deposits and their locations suggest that these deposits formed from several different hydrothermal systems whose alteration halos overlapped, and not from a single hydrothermal system that migrated through time. Therefore, although deposits in the Hauraki goldfield generally young from north to south, on the local scale there can be significant variability that presumably reflects the complex evolution and spatial overlap of the parent hydrothermal systems.

Although more high-quality data would greatly enhance our knowledge of mineralization in the Hauraki goldfield, the available dates constrain almost 90 percent of the Au recovered from the goldfield (Fig. 3). Deposits from different provinces in the goldfield have different ages, metal endowments, and mineralization styles. The northern province of

the Hauraki goldfield has produced 59,137 kg Au from massive to crustiform veins in the Kuaotunu Subgroup of the Coromandel Group and includes the bonanza-style veins at Coromandel and Thames, as well as minor porphyry-style mineralization (Figs. 2, 3; Christie et al., 2007). The eastern province of the goldfield contains stockwork veins, disseminated mineralization, and veins that occur in rhyolite of the Whitianga Group but has produced only 1,607 kg Au. In contrast, the southern province has produced 307,640 kg Au from colloform to crustiform veins and local stockwork veins that occur predominantly in andesite of the Waiwawa Subgroup of the Coromandel Group (Figs. 2, 3; Christie et al., 2007). Therefore, even though gold mineralization in the Hauraki goldfield began around 16.3 Ma and continued episodically to approximately 1.8 Ma, greater than 80 percent of the Au that has been recovered from the goldfield was deposited in the southern province of the goldfield in the relatively short 0.9 Ma window between 6.9 and 6.0 Ma.

Volcanic and structural evolution

The North Island of New Zealand and the adjacent Pacific region have undergone significant tectonic reorganization in the last 30 Ma. On a large scale, there is wide agreement that volcanism in the North Island of New Zealand was localized along the north- to northwest-trending Northland volcanic arc from around 25 Ma to perhaps as late as 15 Ma (e.g., Hayward et al., 2001; Fig. 8). Furthermore, there is consensus that volcanism migrated from the Coromandel to the Taupo Volcanic Zone after 2 Ma (Briggs et al., 2005), and volcanism is now located along the Tonga-Kermadec-Taupo Volcanic Zone arc (Fig. 8). There is also consensus that volcanic rocks generally young southward in the Coromandel volcanic zone (e.g., Adams et al., 1994; Hayward et al., 2001; Briggs et al., 2005), and the pronounced southward-younging of mineral deposits in the Hauraki goldfield may reflect arc migration
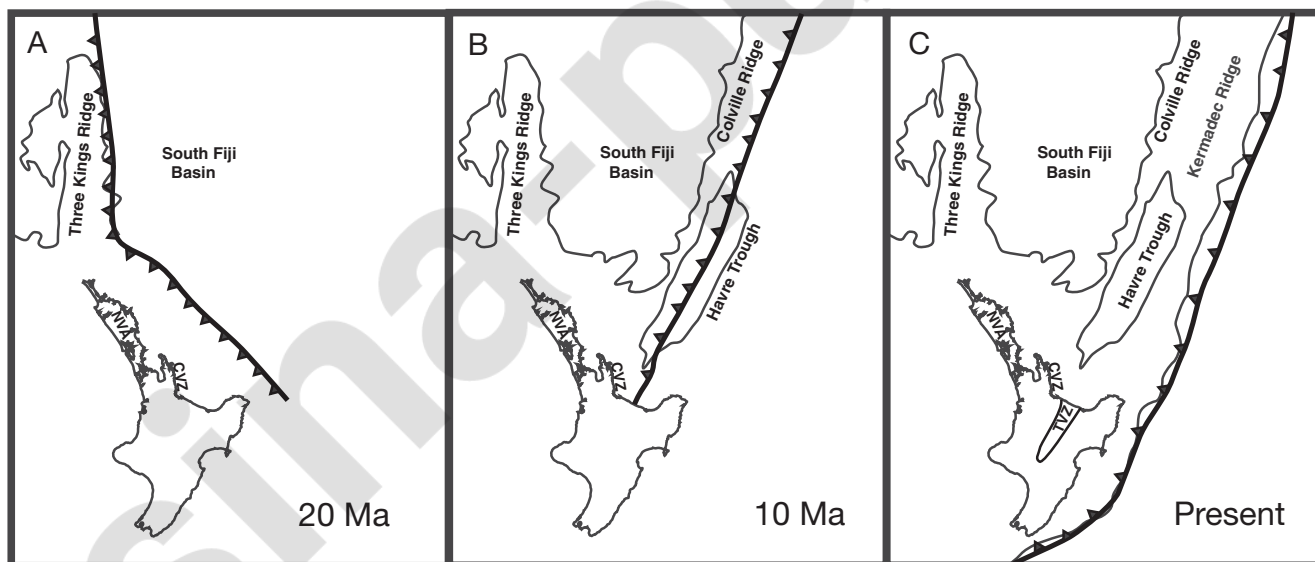

FIG. 8. Generalized map showing the approximate location of arcs in the region of the North Island of New Zealand for the last 20 m.y. Due to the plethora of tectonic reconstructions of New Zealand and the adjacent southwest Pacific, we have not shown a specific reconstruction, but rather use this map to portray, in a general way, the location, migration, and orientation of arcs through time.

from the Colville to the Kermadec ridge (Fig. 1). However, from ca. 20 to 2 Ma, uncertainty and controversy remain for the tectonic, volcanic, and structural evolution of the North Island and the adjacent Pacific region, particularly the evolution of the Three Kings ridge, South Fiji basin, Colville ridge, and Havre trough.

Mortimer et al. (2007) provided new $^{40}Ar/^{39}Ar$ dates of dredge and drill samples from the New Zealand offshore region, show that subduction-related lavas are widespread, and that many of these rocks have early Miocene ages of 22 to 16 Ma. To account for this, the authors propose a west-dipping subduction zone that migrated from the area around the Northland volcanic arc to the area of the Colville ridge around 15 Ma. Dredge samples that were collected from the Colville ridge at 30° to 32°S, more than 800 km from the New Zealand mainland, contain microfossils that indicate that the Colville ridge existed since at least the early Miocene (Ballance et al., 1999). The only rigorous constraint on the timing of volcanism on the Colville arc south of these samples is a K-Ar date of 5.4 Ma from dredged basalt near the southern end of the Colville ridge (Adams et al., 1994). A plagioclase separate of another rock from the same dredge sample was recently dated by $^{40}Ar/^{39}Ar$ and yielded plateau and isochron ages of 16.7 Ma. This new date is regarded as the age of the basalt, and the younger date has been interpreted to reflect hydrothermal alteration of the groundmass (Mortimer et al., 2009). Although most workers accept or imply that the Colville arc was active from early Miocene onward (e.g., Herzer, 1995; Ballance et al., 1999; Mortimer et al., 2007, 2009), there has not yet been detailed systematic testing of volcanic rocks of the Colville arc to compare them with volcanic rocks of the Coromandel volcanic zone to substantiate whether these are indeed part of the same volcanic system nor has there been enough geochronology along the length of the Colville arc to test whether it developed synchronously along its length or whether some segments formed earlier than others.

Therefore, there remain three possibilities for the origin of volcanic rocks of the Coromandel volcanic zone: (1) these rocks are entirely related to the southward migration of the Northland volcanic zone, (2) Coromandel volcanic zone rocks are a product of onshore volcanism from the Colville arc (e.g., Herzer, 1995; Ballance et al., 1999; Mortimer et al., 2007, 2009), or (3) volcanic rocks from the Coromandel volcanic zone are the product of both arcs (Brathwaite and Skinner, 1997). Critical testing of these possibilities awaits detailed petrogenetic studies and geochemical modeling of the interrelationships of the volcanic rocks from these three arcs. In spite of these uncertainties, available data, as summarized below, lead us to favor possibility (3), that volcanic rocks from the Coromandel volcanic zone are the product of both the Northland and Colville arcs, and that reorganization of these arcs may have facilitated the burst of Au-Ag mineralization in the Hauraki goldfield from 6.9 to 6.0 Ma.

The veins in the Hauraki goldfield fill low-displacement faults, and therefore the strike direction of veins in the Hauraki goldfield provides some constraints on the likely orientation of regional stress fields during vein formation and Au-Ag mineralization. Veins in the northern province predominantly strike northwest to northeast and many have north-northwest

to north-south strikes (Fig. 2). If the controlling structures formed parallel to the orientation of the volcanic arc, as is common worldwide (e.g., Rowland and Sibson, 2004; Sillitoe, 2010), then their orientation is most consistent with vein formation as part of the north-northwest–trending Northland volcanic arc. In contrast, most veins in the southern and eastern provinces strike northeast, which is more consistent with vein formation in an arc setting that was parallel to the Colville volcanic arc. The most noteworthy exception is the Ohui deposit in the eastern province, which is the oldest deposit (8.3 Ma) in the eastern and southern goldfields; it contains veins that strike both north-northeast and northwest (Brathwaite et al., 2001a; Fitzgerald et al., 2006).

Structural analyses of epithermal deposits can provide information about the nature and direction of vein opening on the deposit scale, and where these data are relatively consistent from deposit to deposit, regional stress fields can be inferred. There are few structural analyses of deposits from the northern province of the Hauraki goldfield, but data from the southern and eastern provinces of the goldfield indicate that most veins opened in extensional settings; evidence for strike-slip and reverse faults is rare (Spörli et al., 2006). The Broken Hills deposit contains north-south–striking veins that have kinematic indicators that reflect normal dip-slip movement, consistent with formation in an extensional environment (Nortje et al., 2003, 2006). At Golden Cross, the main vein that was mined underground is the Empire vein, which strikes northeast, dips steeply to the northwest, and formed in an extensional setting (Begbie et al., 2007). Veins at Sovereign and Jubilee strike northeast, and available kinematic data indicate that they formed in an extensional setting (Grodzicki et al., 2007). Similarly, the veins at Karangahake strike northeast, dip steeply, and formed in a northwest-southeast extensional environment (Smith et al., 2003). Veins at the world-class Martha deposit at Waihi predominantly strike northeast and also formed in a northwest-southeast extensional environment (Spörli and Cargill, 2011). Finally, the recently discovered Favona deposit has north-northeast–striking veins, and available kinematic data indicate that these veins also formed in an extensional environment (Mortimer, 2009). Taken together, the results strongly indicate regional northwest-southeast extension in the Hauraki goldfield from 7.1 to 6.0 Ma, coincident with the majority of ore deposition in the entire Hauraki goldfield.

Onshore and offshore data provide complementary and consistent records of volcanic activity in the Coromandel volcanic zone. Volcanism in the zone began approximately 18 Ma and was primarily characterized by eruption of andesite of the Kuaotunu Subgroup of the Coromandel Group until approximately 10 to 11 Ma (e.g., Skinner, 1986; Adams et al., 1994; Hayward et al., 2001; Figs. 2, 3). Some workers interpret the Kuaotunu Subgroup as the southern end of the north-northwest–trending Northland volcanic arc (e.g., Hayward et al., 2001), whereas others postulate that the Kuaotunu Subgroup formed in an arc that followed the north-northeast–trending Colville ridge (e.g., Mortimer et al., 2007). Around 10.5 to 10 Ma, volcanism in the Coromandel volcanic zone changed from mostly erupting andesite to a more complex bimodal system that erupted andesite and rhyolite with minor basalt (e.g., Skinner, 1986; Adams et al., 1994; Hayward et al., 2001;

Carter et al., 2003; Fig. 3). Prior to 10 Ma, andesitic rocks of the Kuaotunu Subgroup gradually evolved toward more differentiated compositions, but the onset of andesitic volcanism of the Waiwawa Subgroup led to a return to a more basic chemistry of the andesitic volcanic rocks (Booden et al., 2007). Therefore, available data clearly indicate that the change in style of mineralization from the northern goldfield, where bonanza-style veins are more common, to the southern and eastern goldfield, where thick colloform-crustiform veins are the typical orebodies, coincides with a change from predominantly andesitic volcanism to bimodal andesite-rhyolite eruptive products.

Taken together, the available data lead us to prefer a model that most simply and fully accounts for (1) the change in volcanism from mostly andesite prior to 10 Ma to bimodal andesite and rhyolite with minor basalt thereafter, (2) the change in strike directions of veins from northwest- to northeast striking in the northern province of the goldfield to northeast striking in the southern and eastern provinces, and (3) regional northwest-southeast extension in the southern and eastern provinces after 10 Ma. Of the tectonic hypotheses listed above, the first is that volcanic rocks of the Coromandel volcanic zone are entirely related to the southward migration of the Northland volcanic zone. We agree with other authors that available data indicate that the Colville arc must have interacted with the North Island of New Zealand (e.g., Herzer, 1995; Ballance et al., 1999; Mortimer et al., 2007, 2009), and therefore we reject this first hypothesis. The second hypothesis states that all Coromandel volcanic zone rocks are a product of onshore volcanism from the Colville arc (e.g., Herzer, 1995; Ballance et al., 1999; Mortimer et al., 2007, 2009). This hypothesis could account for the observed change in volcanic style at 10 Ma by change in the dip of the subduction zone or some other mechanism but cannot readily account for the change in the strike directions of veins in the goldfield. The third hypothesis, that volcanic rocks from the Coromandel volcanic zone are the product of both arcs (cf. Brathwaite and Skinner, 1997; Hayward et al., 2001) can account for the change in composition of volcanism, the change in strike directions, and regional extension in the southern and eastern provinces. Therefore, although more work is needed, we prefer a hypothesis that correlates the change in volcanism, mineralization style, and structural orientations of the veins in the Hauraki goldfield with reorganization of the Northland and Colville arcs. We agree with other authors that the Colville arc was active elsewhere along its length prior to 10 Ma (e.g., Herzer, 1995; Ballance et al., 1999; Mortimer et al., 2007, 2009), but we suggest that in the Coromandel volcanic zone, reorganization of the Northland and Colville arcs may have occurred just before the onset of Whitianga Group rhyolite volcanism at approximately 10 Ma.

The greatest pulse of Au deposition in the Hauraki goldfield occurred between 6.9 and 6.0 Ma and was preceded from ca. 9 to 7 Ma by significant volcanism, including major ignimbrite eruptions and caldera collapse (Adams et al., 1994). This episode was followed by significant eruption of rhyolite, including ignimbrite from ca. 6 to 5 Ma (Skinner, 1986; Brathwaite and Christie, 1996). These data suggest that the most significant phase of ore formation appears to coincide with a relatively quiescent phase of volcanism between

ca. 7 and 6 Ma in the onshore record (Adams et al., 1994), and between 7.0 and 6.3 Ma in the Pacific tephra record (Carter et al., 2003). Unfortunately, the time constraints of this apparent quiescent period remain somewhat uncertain because the onshore dates were acquired by whole-rock K-Ar methods, and hydrothermal alteration that can readily perturb igneous ages is common and widespread (e.g., Mauk and Simpson, 2007; Booden et al., 2011). Therefore, although it appears that the greatest pulse of mineralization in the Hauraki goldfield coincided with a relatively quiescent period during bimodal andesite-rhyolite volcanism, the evidence for the exact timing of quiescence is less certain.

In spite of these uncertainties, it is clear that Au deposition in the Hauraki goldfield coincides, in the broadest sense, with reorganization of major volcanic arcs in the New Zealand region of the southwest Pacific (Brathwaite and Skinner, 1997). Furthermore, Au deposition was not consistent through time but instead was restricted to certain periods of the volcanic history of the Coromandel volcanic zone. The available data strongly indicate that Au deposition in the southern Hauraki goldfield, which accounts for greater than 80 percent of the Au endowment of the entire goldfield, was focused on a 0.9 Ma time interval that coincided with regional extension. Presumably, this extension facilitated several million years of eruption of large volumes of rhyolite and lesser basalts. In turn, this voluminous volcanic activity elevated heat flow, which helped enhance hydrothermal fluid circulation and epithermal mineralization (Fig. 3).

Conclusions

Epithermal gold mineralization in the Hauraki goldfield of New Zealand formed between 16.3 and 1.8 Ma in an area where volcanism changed from andesite-dominant to bimodal andesite-rhyolite at approximately 10 Ma. Our high precision $^{40}Ar/^{39}Ar$ and Re-Os results indicate that mineralization in the Hauraki goldfield also evolved in two discrete stages, with a transition from mineralization in the northern to the southern and eastern goldfields at approximately 10 Ma, and deposits progressively young in a northwest-southeast direction. This younging likely reflects, at least in part, the migration of volcanism from the Colville to the Kermadec ridge (Fig. 1). The goldfield has produced greater than 320,000 kg Au and 1.5 Mkg Ag (Christie et al., 2007), but more than 80 percent of the gold was deposited in a short 0.9 Ma window that occurred during the 10 to 4 Ma period of productive bimodal volcanism (Fig. 3). However, the actual window of most prolific Au mineralization, from 6.9 to 6.0 Ma, appears to correlate with a general lull in volcanism.

Therefore, even though volcanism in the Coromandel volcanic zone spanned an interval from 18 to 2 Ma, the gold endowment of the Hauraki goldfield did not build gradually and steadily through time, but rather most known gold mineralization was deposited in a brief time interval of less than 1 m.y. Understanding the controls that help focus mineralization in time and whether mineralization was continuous or episodic remain outstanding and unresolved research questions. Nonetheless, the most productive period of mineralization coincides with regional extension and bimodal volcanism that might be a product of post-11 Ma reorganization of the Colville and Northland volcanic arcs—the two major arcs that

produced Miocene volcanic rocks in the New Zealand region of the southwest Pacific.

Acknowledgments

REFERENCES

Adams, C.J., Graham, I.J., Seward, D., and Skinner, D.N.B., 1994, Geochronological and geochemical evolution of late Cenozoic volcanism in the Coromandel peninsula, New Zealand: New Zealand Journal of Geology and Geophysics, v. 37, p. 359–379.

Albinson, T., Norman, D.I., Cole, D., and Chomiak, B., 2001, Controls on formation of low-sulfidation epithermal deposits in Mexico: Constraints from fluid inclusion and stable isotope data: Society of Economic Geologists Special Publication 8, p. 1–32.

Ballance, P.F., 1999, Simplification of the Southwest pacific Neogene arcs: Inherited complexity and control by a retreating pole of rotation: Geological Society of London Special Publication 164, p. 7–19.

Ballance, P.F., Ablaev, A.G., Pushchin, I.K., Pletnev, S.P., Birylina, M.G., Itaya, T., Follas, H.A., and Gibson, G.W., 1999, Morphology and history of the Kermadec trench-arc-backarc basin-remnant arc system at 30 to 32°S: Geophysical profile, microfossil and K–Ar data: Marine Geology, v. 159, p. 35–62.

Barra, F., Ruiz, J., Mathur, R., and Titley, S., 2003, A Re-Os study on sulfide minerals from the Bagdad porphyry Cu-Mo deposit, northern Arizona, United States: Mineralium Deposita, v. 38, p. 585–596.

Bates, T.E., 1989, Te Aroha goldfield—Tui and Waiorongomai gold/silver/base metal prospects: Australasian Institute of Mining and Metallurgy Monograph 13, p. 79–81.

Begbie, M.J., Spörli, K.B., and Mauk, J.L., 2007, Structural evolution of the Golden Cross epithermal Au-Ag deposit, New Zealand: Economic Geology, v. 102, p. 873–892.

Birck, J.L., RoyBarman, M., and Capmas, F., 1997, Re-Os measurements at the femtomole level in natural samples: Geostandard Newsletter, v. 20, p. 19–27.

Booden, M.A., Mauk, J.L., Briggs, R.M., and Brathwaite, R.L., 2007, Geochemistry of volcanism in the Miocene-Pliocene Hauraki volcanic region, North Island [abs.]: Geological Society of New Zealand and New Zealand Geophysical Society Joint Annual Conference, Programme and Abstracts, p. 18.

Booden, M.A., Mauk, J.L., and Simpson, M.P., 2011, Quantifying metasomatism in epithermal Au-Ag deposits: A case study from the Waitekauri area, New Zealand: Economic Geology, v. 106, p. 999–1030.

Brathwaite, R.L., 1989, Geology and exploration of the Karangahake gold-silver deposit: Australasian Institute of Mining and Metallurgy Monograph 13, p. 73–78.

Brathwaite, R.L., and Christie, A.B., 1996, Geology of the Waihi area, sheet T13BD: Institute of Geological and Nuclear Sciences Geological Map 21, scale 1:50,000 + 64 p.

Brathwaite, R.L., and Faure, K., 2002, The Waihi gold-silver-base metal sulfide-quartz vein system, New Zealand: Temperature and salinity controls on electrum and sulfide deposition: Economic Geology, v. 97, p. 269–290.

Brathwaite, R.L., and Pirajno, F., 1993, Metallogenic map of New Zealand: Institute of Geological and Nuclear Sciences Monograph 3, 215 p.

Brathwaite, R.L., and Skinner, D.N.B., 1997, The Coromandel epithermal gold-silver province: A result of collision of the Northland and Colville volcanic arcs in northern New Zealand: New Zealand Minerals and Mining Conference, 1997, Publicity Unit, Crown Minerals, Ministry of Commerce, Proceedings, p. 111–117.

Brathwaite, R.L., Cargill, H.J., Christie, A.B., and Swain, A., 2001a, Lithological and spatial controls on the distribution of quartz veins in andesite- and rhyolite-hosted epithermal Au-Ag deposits of the Hauraki goldfield, New Zealand: Mineralium Deposita, v. 36, p. 1–12.

Brathwaite, R.L., Simpson, M.P., Faure, K., and Skinner, D.N.B., 2001b, Telescoped porphyry Cu-Mo-Au mineralisation, advanced argillic alteration and quartz-sulphide-gold-anhydrite veins in the Thames district, New Zealand: Mineralium Deposita, v. 36, p. 623–640.

Brathwaite, R.L., Torckler, L.K., and Jones, P.K., 2006, The Martha Hill epithermal Au-Ag deposit, Waihi—geology and mining history: Australasian Institute of Mining and Metallurgy Monograph 25, p. 171–178.

Briggs, R.M., Houghton, B.F., McWilliams, M., and Wilson, C.N.J., 2005, ^{40}Ar/^{39}Ar ages of silicic volcanic rocks in the Tauranga-Kaimai area, New Zealand: Dating the transition between volcanism in the Coromandel arc and the Taupo Volcanic Zone: New Zealand Journal of Geology and Geophysics, v. 48, p. 459–469.

CANZ, 1996, "Undersea New Zealand" (New Zealand Region Physiography), 1:4 000,000, 2nd ed.: New Zealand Oceanographic Institute (now NIWA) Chart, Miscellaneous Series 74.

Carman, G.D., 2003, Geology, mineralization, and hydrothermal evolution of the Ladolam gold deposit, Lihir Island, Papua New Guinea: Society of Economic Geologists Special Publication 10, p. 247–284.

Carter, L., Shane, P., Alloway, B., Hall, I.R., Harris, S.E., and Westgate, J.A., 2003, Demise of one volcanic zone and birth of another—a 12 m.y. marine record of major rhyolitic eruptions from New Zealand: Geology, v. 31, p. 493–496.

Cartwright, A.J., 1982, Geology of Waiorongamai Valley, Te Aroha: Unpublished M.Sc. thesis, Auckland, New Zealand, University of Auckland, 163 p.

Christie, A.B., Rabone, S.D.C., Barker, R.G., and Merchant, R.J., 2006, Exploration of the Wharekiraupongo epithermal Au-Ag deposit, Hauraki goldfield: Australasian Institute of Mining and Metallurgy Monograph 25, p. 137–144.

Christie, A.B., Simpson, M.P., Brathwaite, R.L., Mauk, J.L., and Simmons, S.F., 2007, Epithermal Au-Ag and related deposits of the Hauraki goldfield, Coromandel volcanic zone, New Zealand: Economic Geology, v. 102, p. 785–816.

Edbrooke, S.W., comp., 2001, Geology of the Auckland area: Institute of Geological and Nuclear Sciences 1:250,000 Geological Map 3.

Fitzgerald, M.J., Briggs, R.M., and Grieve, P.L., 2006, Exploration and geology of the Ohui epithermal Au-Ag prospect, Hauraki goldfield: Australasian Institute of Mining and Metallurgy Monograph 25, p. 191–194.

Grodzicki, K.R., Mauk, J.L., McConnochie, R., and Rowland, J.V., 2007, Structural geology of the Sovereign prospect, lower Waitekauri Valley, Hauraki goldfield, New Zealand: Annual Conference of the New Zealand Branch of the AusIMM, 40th, Proceedings, p. 103–108.

Hall, C.M., and Farrell, J.W., 1995, Laser ^{40}Ar/^{39}Ar ages of tephra from Indian Ocean deep-sea sediments: Tie points for the astronomical and geomagnetic polarity time scales: Earth and Planetary Science Letters, v. 133, p. 327–338.

Haworth, A.V., and Briggs, R.M., 2006, Epithermal Au-Ag mineralisation in the lower Waitekauri Valley, Hauraki goldfield: Australasian Institute of Mining and Metallurgy Monograph 25, p. 157–162.

Hayward, B.W., Black, P.M., Smith, I.E.M., Ballance, P.F., Itaya, T., Doi, M., Takagi, M., Bergman, S., Adams, C.J., Herzer, R.H., and Robertson, D.J., 2001, K-Ar ages of early Miocene arc-type volcanoes in northern New Zealand: New Zealand Journal of Geology and Geolphysics, v. 44, p. 285–311.

Hayward, B.W., Grenfell, H.R., Mauk, J.L., and Moore, P.R., 2006, The west-flowing Pliocene "Clevedon River," Auckland: Geological Society of New Zealand Newsletter v. 141, p. 24–29.

Henry, C.D., Elson, H.B., McIntosh, W.C., Heizler, M.T., and Castor, S.B., 1997, Brief duration of hydrothermal activity at Round Mountain, Nevada, determined from $^{40}Ar/^{39}Ar$ geochronology: Economic Geology, v. 92, p. 807–826.

Herzer, R.H., 1995, Seismic stratigraphy of a buried volcanic arc, Northland, New Zealand, and implications for Neogene subduction: Marine and Petroleum Geology, v. 12, p. 511–533.

Hochstein, M.P., and Ballance, P.F., 1993, Hauraki rift: A young, active, intra-continental rift in a back-arc setting, in South Pacific sedimentary basins, sedimentary basins of the world: Elsevier, Amsterdam, 2, p. 295–305.

Hochstein, M.P., Tearney, K., Rawson, K., Davey, F.J., Davidge, S., Henrys, S., and Backshall, D., 1986, Structure of the Hauraki rift (New Zealand): Royal Society of New Zealand Bulletin, v. 24, p. 333–348.

Houghton, B.F., and Cuthbertson, A.S., 1989, Geological map of New Zealand 1:50,000, sheet T14 BD Kaimai: Wellington, Department of Scientific and Industrial Research.

Hunt, P.A., and Roddick, J.C., 1992, A compilation of K-Ar and ^{40}Ar-^{39}Ar ages, Report 22: Geological Survey of Canada Paper 92-2, p. 179–226.

——1993, A compilation of K-Ar and ^{40}Ar-^{39}Ar ages, Report 7: Geological Survey of Canada Paper 93-2, p. 127–154.

Izawa, E., Urashima, Y., Ibaraki, K., Suzuki, R., Yokoyama, T., Kawasaki, K., Koga, A., and Taguchi, S., 1990, The Hishikari gold deposit: High-grade epithermal veins in Quaternary volcanics of southern Kyushu, Japan: Journal of Geochemical Exploration, v. 36, p. 1–56.

John, D.A., 2001, Miocene and early Pliocene epithermal gold-silver deposits of the northern Great Basin, western United States: Characteristics, distribution, and relationship to magmatism: Economic Geology, v. 96, p. 1827–1853.

Leavitt, E.D., Spell, T.L., Goldstrand, P.M., and Arehart, G.B., 2004, Geochronology of the Midas low-sulfidation epithermal gold-silver deposit, Elko County, Nevada: Economic Geology, v. 99, p. 1665–1686.

Locke, C.A., Morrell, A.E., Cassidy, J., and Smith, N., 2006, Magnetic and gravity methods in the exploration of epithermal deposits in the Coromandel peninsula, Hauraki goldfield: Australasian Institute of Mining and Metallurgy Monograph 25, p. 95–100.

Main, J.V., 1971, Geology of the Maratoto-Waipaheke area, Coromandel peninsula: Unpublished M.Sc. thesis, Auckland, New Zealand, University of Auckland, 171 p.

——1979, Precious metal bearing veins of the Maratoto-Wentworth area, Hauraki goldfield, New Zealand: New Zealand Journal of Geology and Geophysics, v. 22, p. 41–51.

Mauk, J.L., and Hall, C.M., 2004, $^{40}Ar/^{39}Ar$ ages of adularia from the Golden Cross, Neavesville and Komata epithermal deposits, Hauraki goldfield, New Zealand: New Zealand Journal of Geology and Geophysics, v. 47, p. 227–231.

Mauk, J.L., and Simpson, M.P., 2007, Geochemistry and stable isotope composition of altered rocks at the Golden Cross epithermal Au-Ag deposit, New Zealand: Economic Geology, v. 102, p. 841–871.

Mauk, J.L., Kyle, J.R., Simpson, M.P., and Atkinson, P., 2006a, Ore mineralogy of the BM37 shoot of the Karangahake deposit, New Zealand: Annual Conference of the New Zealand Branch of the Australasian Institute of Mining and Metallurgy, 39th, Proceedings, p. 233–242.

Mauk J.L., Simpson M.P., Hollinger H., Morrell A.E., Smith N., Locke C.A., and Cassidy J., 2006b, The Favona epithermal Au-Ag deposit, Hauraki goldfield—mineralogy, geochemistry and geophysics: Australasian Institute of Mining and Metallurgy Monograph 25, p. 185–190.

Merchant, R.J., 1986, Mineralisation in the Thames district, Coromandel, in Henley, R.W., Hedenquist, J.W., and Roberts P.J., eds., Guide to active epithermal (geothermal) systems and precious metal deposits of New Zealand: Berlin, Gebrüder Bornträger, Monograph Series Mineral Deposits 26, p. 165–183.

Moore, C.R., 1979, Geology and mineralisation of the former Broken Hills gold mine, Hikuai, Coromandel, New Zealand: New Zealand Journal of Geology and Geophysics, v. 22, p. 339–351.

Morrell, A.E., Locke, C.A., Cassidy, J., and Mauk, J.L., 2011, Geophysical characteristics of adularia-sericite epithermal gold-silver deposits in the Waihi-Waitekauri region, New Zealand: Economic Geology, v. 106, p. 1031–1041.

Mortimer, J.A., 2009, Kinematic indicators of vein opening at the Favona epithermal Au-Ag deposit, Waihi, New Zealand: Australasian Institute of Mining and Metallurgy New Zealand Branch Annual Conference 2009, Proceedings, p. 293–303.

Mortimer, N., Herzer, R.H., Gans, P.B., Laporte-Magoni, C., Calvert, A.T., and Bosch, D., 2007, Oligocene-Miocene tectonic evolution of the South Fiji basin and Northland plateau, SW Pacific Ocean: Evidence from petrology and dating of dredged rocks: Marine Geology, v. 237, p. 1–24.

Mortimer, N., Gans, P.B., Palin, J.M., Meffre, S., Herzer, R.H., and Skinner, D.N.B., 2010, Location and migration of Miocene-Quaternary volcanic arcs in the SW Pacific region: Journal of Volcanology and Geothermal Research, v. 190, p. 1–10.

Nägler, T.F., and Frei, R., 1997, Plug in plug osmium distillation: Schweizerische Mineralogische Petrographische Mitteilungen, v. 77, p. 123–127.

Nortje, G.S., Rowland, J., Mauk, J.L., and Rabone, S.D.C., 2003, Structural controls on mineralisation at the Broken Hills epithermal Au-Ag deposit, Coromandel peninsula, New Zealand: New Zealand Branch of the AusIMM Annual Conference, Proceedings, p. 271–280.

Nortje, G.S., Rowland, J., Spörli, K.B., Blenkinsop, T.G., and Rabone, S.D.C., 2006, Vein deflections and thickness variations of epithermal quartz veins as indicators of fracture coalescence: Journal of Structural Geology, v. 28, p. 1396–1405.

Panther, C.A., 1996, Textural, mineralogical and geochemical relationships within epithermal veins at the Martha Hill Au-Ag deposit, Waihi, New Zealand: Unpublished M.Sc. thesis, Auckland, New Zealand, University of Auckland, 122 p.

Rabone, S.D.C., 1991, Residual total force magnetic anomaly map, Coromandel region: New Zealand Geological Survey Report M183.

——2006a, Broken Hills rhyolite-hosted high level epithermal vein system, Hauraki goldfield—100 years on: Australasian Institute of Mining and Metallurgy Monograph 25, p. 117–122.

——2006b, Exploration at Te Puke, Hauraki goldfield—the last 30 years: Australasian Institute of Mining and Metallurgy Monograph 25, p. 191–194.

Rabone, S.D.C., Moore, D.H., and Barker, R.C., 1989, Geology of the Wharekirauponga epithermal gold deposit, Coromandel region: Australasian Institute of Mining and Metallurgy Monograph 25, p. 93–99.

Richards, J.P. and Noble, S.R., 1998, Application of radiogenic isotope systems to the timing and origin of hydrothermal processes: Reviews in Economic Geology, v. 10, p. 195–233.

Richards, J.R., Cooper, J.A., and Black, P.M., 1966, Potassium-argon age of plutonic intrusives on Cape Colville peninsula and Cuvier Island, New Zealand: Nature, v. 211, p. 725–726.

Rowland, J.V., and Sibson, R.H., 2004, Structural controls on hydrothermal flow in a segmented rift system, Taupo Volcanic Zone, New Zealand: Geofluids, v. 4, p. 259–283.

Sanematsu, K., Watanabe, K., Duncan, R.A., and Izawa, E., 2006, The history of vein formation determined by $^{40}Ar/^{39}Ar$ dating of adularia in the Hosen-1 vein at the Hishikari epithermal gold deposit, Japan: Economic Geology, v. 101, p. 685–698.

Saunders, J.A., Unger, D.L., Kamenov, G.D., Fayek, M., Hames, W.E., and Utterback, W.C., 2008, Genesis of middle Miocene Yellowstone hotspot-related bonanza precious Au-Ag deposits, Northern Great Basin, USA: Mineralium Deposita, v. 43, p. 715–734.

Sillitoe, R.H., 2008, Major gold deposits and belts of the North and South America Cordillera: Distribution, tectonomagmatic settings, and metallogenic considerations: Economic Geology, v. 103, p. 663–687.

——2010, Porphyry copper systems: Economic Geology, v. 105, p. 3–41.

Simmons, S.F., and Browne, P.R.L., 2000, Hydrothermal minerals and precious metals in the Broadlands-Ohaaki geothermal system: Implications for understanding low-sulfidation epithermal environments: Economic Geology, v. 95, p. 971–999.

Simmons, S.F., White, N.C., and John, D.A., 2005, Geological characteristics of epithermal precious and base metal deposits: Economic Geology 100th Anniversary Volume, p. 485–522.

Simpson, M.P., and Mauk, J.L., 2007, The Favona epithermal gold-silver deposit, Waihi, New Zealand: Hydrothermal alteration, hydrologic evolution and implications for exploration: Economic Geology, v. 102, p. 817–839.

——2011, Hydrothermal alteration and veins at the epithermal Au-Ag deposits and prospects of the Waitekauri area, Hauraki goldfield, New Zealand: Economic Geology, v. 106, p. 945–973.

Simpson, M.P., Mauk, J.L., and Simmons, S.F., 2001, Hydrothermal alteration and hydrologic evolution of the Golden Cross epithermal Au-Ag deposit, New Zealand: Economic Geology, v. 96, p. 773–796.

Sinsuat, O.A., 1992, Epithermal mineralization and alteration in the Thames-Waiomu area, Coromandel peninsula, New Zealand: Unpublished M.Sc. thesis, Auckland, New Zealand, University of Auckland, 138 p.

Skinner, D.N.B., 1972, Subdivision and petrology of the Mesozoic rocks of the Coromandel (Manaia Hill Group): New Zealand Journal of Geology and Geophysics, v. 15, p. 203–227.

——1976, Geological map of New Zealand 1:63,360, sheet N40 and part sheets N35, N36 and N39—northern Coromandel: Wellington, Department of Scientific and Industrial Research.

——1986, Neogene volcanism of the Hauraki volcanic region: Royal Society of New Zealand Bulletin, v. 23, p. 21–47.

Smith, S.F., Rowland, J., and Mauk, J., 2003, Structural control of mineralisation at the Karangahake epithermal Au-Ag deposit, Coromandel peninsula, New Zealand: New Zealand Branch of the Australasian Institute of Mining and Metallurgy Annual Conference, Proceedings, p. 281–290.

Spörli, K.B., and Cargill, H., 2011, Structural evolution of a world-class epithermal orebody: the Martha Hill deposit, Waihi, New Zealand: ECONOMIC GEOLOGY, v. 106, p. 975–998.

Spörli, K.B., Begbie, M.J., Irwin, M.R., and Rowland, J.V., 2006, Structural processes and tectonic controls on the epithermal Au-Ag deposits of the Hauraki goldfield: Australasian Institute of Mining and Metallurgy Monograph 25, p. 85–94.

Steiger, R.H., and Jäger, E., 1977, Subcommission on geochronology; convention on the use of decay constants in geo- and cosmochronology: Earth and Planetary Science Letters, v. 36, p. 359–362.

Stevens, M.R., and Boswell, G.B., 2006, Review of exploration and geology of the Karangahake Au-Ag deposit, Hauraki goldfield: Australasian Institute of Mining and Metallurgy Monograph 25, p. 163–171.

Stuart, A.G.J., 2006, Hydrothermal alteration and geochemistry of the Karangahake adularia-sericite epithermal Au-Ag deposit, Hauraki goldfield, New Zealand: Unpublished M.Sc. thesis, Auckland, New Zealand, University of Auckland, 152 p.

Sumantri, T.A.F., 1991, Structure, hydrothermal alteration and geochemistry of the Karangahake epithermal vein system, Karangahake, New Zealand: Unpublished M.Sc. thesis, Auckland, New Zealand, University of Auckland, 157 p.

Torckler, L.K., McKay, D., and Hobbins, J., 2006, Geology and exploration of the Favona Au-Ag deposit, Waihi, Hauraki goldfield: Australasian Institute of Mining and Metallurgy Monograph 25, p. 179–184.

Ward, K.T., Mauk, J.L., and Hall, C., 2005. New ^{40}Ar/^{39}Ar dates of adularia from epithermal deposits in the Hauraki goldfield, New Zealand: New Zealand Minerals Conference, Crown Minerals, 2005, Ministry of Economic Development and Australasian Institute of Mining and Metallurgy, New Zealand Branch, Proceedings, p. 426–433.

Wellman, H.W., 1954, Stress formation controlling lode formation and faulting at Waihi mine and notes on the stress pattern in the northwestern part of the North Island of New Zealand: New Zealand Journal of Science and Technology, v. 36B, p. 201–206.

Wendt, I., and Carl, C., 1991, The statistical distribution of the mean squared weighted deviation: Chemical Geology (Isotope Geoscience section), v. 86, p. 275–285.

APPENDIX

Sample Descriptions

(AU refers to the Auckland University sample numbers, and MC and MI refer to Chris Hall analytical numbers. Grid References (GR.) are in New Zealand Map Grid)

Broken Hills

AU 56756 (MC07-S16) (GR. N 6,451,275; E 2,754,050)
Coarse adularia crystals from colloform-crustiform banded quartz vein from the Night Reef at the battery level at Broken Hills. Sample provided by Stuart Rabone. Adularia extracted to obtain ^{40}Ar/^{39}Ar dates.

AU 56757 (MC07-S17) (GR. N 6,451,275; E 2,754,050)
Coarse adularia crystals from colloform-crustiform banded quartz vein from the Night Reef at the battery level at Broken Hills. Sample provided by Stuart Rabone. Adularia extracted to obtain ^{40}Ar/^{39}Ar dates.

Eliza

AU 59722 (MC24-m3) (GR. N 6,392,550; E 2,762,265)
Massive to weakly banded quartz vein with minor adularia along some bands. Sample provided by Newmont Waihi Gold. Adularia extracted to obtain ^{40}Ar/^{39}Ar dates.

Favona (Moonlight)

AU 55007 (MI91-G26) (GR. 6419389 N; 2763752 E)
Quartz vein with adularia from drill hole UW 57 435m from the Moonlight deposit. Adularia extracted to obtain ^{40}Ar/^{39}Ar dates.

Jubilee and/or Scotia

AU 59720 (MC24-m6a) (GR. N 6,420,974; E 2,754,833)
Sample is from a 1- to 2-mm-wide adularia veinlet from drill hole WV006 at 351.95-m depth from the area between the Jubilee and Scotia deposits (cf. Simpson and Mauk, 2011). Adularia extracted to obtain ^{40}Ar/^{39}Ar dates.

Karangahake

AU 43566 (MC07-S28) (GR. N 6,415,800; E 2,751,100)
Adularia from banded quartz vein; center of the sample has coarse euhedral quartz, and sample margins have colloform banded quartz with adularia. Quartz vein hosted by highly silicified andesite at the 8th level of Karangahake (Sumantri, 1991). Adularia extracted to obtain ^{40}Ar/^{39}Ar dates.

AU 43582 (MC07-S27) (GR. N 6,415,800; E 2,751,100)
White blueish, brecciated quartz vein from the 8th level of Karangahake, approximately 255m north of Kelliors X-cut (Sumantri, 1991). Adularia extracted to obtain ^{40}Ar/^{39}Ar dates.

AU 57488 (MC07-S26) (GR. N 6,414,877; E 2,751,631)
Andesite breccia with intense and pervasive potassic alteration collected from the 8th level of the Karangahake deposit, adjacent to the Welcome lode, where the Welcome stope intersects the Keillors crosscut. Adularia completely replaces igneous plagioclase, and illite partially replaces adularia (Stuart, 2006). Adularia extracted to obtain ^{40}Ar/^{39}Ar dates.

Maratoto

AU 18165 (MC07-S14) (GR. N 6,428,600; E 2,755,000)
Quartz vein with silver mineralization collected from the 3rd level stope of the Maratoto deposit (Main, 1971). NZ map grid coordinates are approximate. Adularia extracted to obtain ^{40}Ar/^{39}Ar dates.

AU 18172 (MC07-S13) (GR. N 6,428,600; E 2,755,000)
Quartz vein with silver mineralization collected from the 2nd to 3rd level winze of the Maratoto deposit (Main, 1971). NZ map grid coordinates are approximate. Adularia extracted to obtain ^{40}Ar/^{39}Ar dates.

AU 18176 (MC07-S15) (GR. N 6,428,600; E 2,755,000)
Quartz vein with silver mineralization collected from the 2nd to 3rd intermediate level of the Maratoto deposit (Main, 1971). NZ map grid coordinates are approximate. Adularia extracted to obtain ^{40}Ar/^{39}Ar dates.

Martha

AU 46851 (MI91-G21) (GR. N 6,420,000; E 2,762,000)
Vein breccia from the Welcome lode that contains adularia collected from 1070 RL of the Martha open pit at approximate mine grid 1420 N, 1470 E (Panther, 1996). Adularia extracted to obtain ^{40}Ar/^{39}Ar dates.

AU 46876 (MI91-G19) (GR. N 6,420,000; E 2,762,000)
Andesite host rock with intense and pervasive potassic alteration, located peripheral to quartz veins on the 1045 RL of the Martha open pit at mine grid 1579.5 N, 1615 E (Panther, 1996). Adularia extracted to obtain ^{40}Ar/^{39}Ar dates.

AU 55008 (MI91-G20) (GR. N 6,420,000; E 2,761,900)
Coarse adularia crystals in quartz vein; grab sample from the open pit in the Martha deposit collected by Stuart Simmons. Exact grid reference and depth unknown. Adularia extracted to obtain ^{40}Ar/^{39}Ar dates.

AU 55009 (MI91-G25) (GR. N 6,420,000; E 2,761,900)
Adularia from wall rock with intense and pervasive potassic alteration adjacent to quartz vein; grab sample collected by Mark Simpson from the 1035 level of the open pit in the Martha deposit at approximate mine grid 1465 N, 1410 E. Adularia extracted to obtain ^{40}Ar/^{39}Ar dates.

AU 55010 (MI91-G27) (GR. N 6,420,200; E 2,762,202)
Sample is silicified andesite with plagioclase completely replaced by adularia and minor illite from drill hole WHD9 202.0m, which is an elevation of –4 m asl (996m RL); main sample in GNS collections, as number P42819. Sample was located 30 m east of the hanging wall of the Martha lode and within the Martha-Welcome vein zone envelope and represents the early stage of vein filling and alteration at Martha (B. Brathwaite, writ. commun., 2010). Adularia extracted to obtain ^{40}Ar/^{39}Ar dates.

AU 59724 (GR. N 6,420,700; E 2,762,700)
Quartz vein with molybdenite from deep levels of the Martha mine; 730 m level in mine, which is 270 m below sea level,

Waihi extension, 1916; main sample in GNS collections (P7915). Molybdenite extracted to obtain Re-Os dates.

AU 59725 (GR. N 6,420,700; E 2,762,700)

Quartz vein with molybdenite from the deep levels of the Martha deposit; main sample at Waihi Arts Centre museum. Exact grid reference and depth unknown. Molybdenite extracted to obtain Re-Os dates.

Muirs Reef

AU 59723 (MC24-m4) (GR. N 6,370,090; E 2,797,821)

Crustiform to colloform banded vein dominated by milky white quartz, with adularia occurring locally in some bands; sample collected from the mine dump from the Muirs Reef deposit. Sample provided by Glass Earth Gold Ltd. Adularia extracted to obtain ^{40}Ar/^{39}Ar dates.

Ohio Creek

AU 59726 (GR. N 6,452,400; E 2,737,200)

Quartz vein with molybdenite from porphyry deposit near Thames from Ohio Creek DDH 6 at 337.9 m-depth, which is approximately 120 m below sea level; main sample in GNS collections (P63205). Quartz vein with molybdenite likely formed toward the end of the first stage of potassic, propylitic and phyllic alteration with associated Cu-Mo-Au mineralization (B. Brathwaite, writ. commun., 2010). Molybdenite extracted to obtain Re-Os dates.

Ohui

AU 59719 (MC24-m5) (GR. N 6,453,100; E 2,765,400)

Adularia crystals approximately 1 mm across in vugs in quartz vein; sample collected from the Phoenix mine dump at the Ohui prospect by Rod Martin. Adularia extracted to obtain ^{40}Ar/^{39}Ar dates.

Opitonui

AU 56760 (MC07-S22) (GR. N 6,487,703; E 2,741,038)

One- to 3-cm-wide vein with coarse-grained quartz and angular clasts of andesite host rock from 107.95-m depth in drill hole OPT-1. Adularia extracted to obtain ^{40}Ar/^{39}Ar dates.

AU 56761 (MC07-S23) (GR. N 6,487,703; E 2,741,038)

One cm-wide vein with coarse-grained quartz from 106.5-m depth in drill hole OPT-1. Adularia extracted to obtain ^{40}Ar/^{39}Ar dates.

AU 56762 (MC07-S24) (GR. N 6,487,703; E 2,741,038)

One- to 3-cm-wide vein with quartz crystals that range up to 5 mm long from 85-m depth in drill hole OPT-1. Adularia extracted to obtain ^{40}Ar/^{39}Ar dates.

Paritu

AU 56763 (MC07-S25) (GR. N 6,515,392; E 2,719,514)

Adularia crystals up to 4 mm across in a vug in a quartz vein. Sample collected by Rod Martin from biotite quartz oligoclase hornfels margin that was described as druse by Skinner (1976). Adularia extracted to obtain ^{40}Ar/^{39}Ar dates.

Sovereign

AU 56758 (MC07-S20) (GR. N 6,420,544; E 2,754,267)

Andesitic host rock with strong potassic alteration from DDH ML 11 at 77.4-m depth at the Sovereign prospect (Simpson and Mauk, 2011). Adularia extracted to obtain ^{40}Ar/^{39}Ar dates.

AU 56759 (MC07-S21) (GR. N 6,420,481; E 2,754,337)

Andesitic host rock with strong potassic alteration from DDH ML1: 111.9-m depth at the Sovereign prospect (Simpson and Mauk, 2011). Adularia extracted to obtain ^{40}Ar/^{39}Ar dates.

AU 59721 (MC24-m7) (GR. N 6,420,544; E 2,754,267)

Quartz veinlet with local adularia from DDH ML11 at 292.8-m depth at the Sovereign prospect (Simpson and Mauk, 2011). Adularia extracted to obtain ^{40}Ar/^{39}Ar dates.

Waiorongomai

AU 33870 (MC07-S18) (GR. N 6,402,000; E 2,753,400)

Massive vein with coarse-grained quartz and minor adularia. Sample collected from the Big Buck Reef at the middle level tramway, Waiorongomai Valley (Cartwright, 1982). Adularia extracted to obtain ^{40}Ar/^{39}Ar dates.

AU 33973 (MC07-S19) (GR. N 6,403,800; E 2,753,600)

Crustiform banded quartz vein with mostly coarse grained quartz, and one band that is rich in base metal sulfides. Local colloform banding; adularia is associated with colloform-banded quartz. Sample collected from the Hero vein, which occurs adjacent the Big Buck Reef in upper Premier Creek, Waiorongomai Valley (Cartwright, 1982). Adularia extracted to obtain ^{40}Ar/^{39}Ar dates.

Wharekirauponga

AU 56755 (MC07-S29) (GR. N 6,430,240; E 2,760,152)

Colloform banded quartz vein with local adularia hosted by rhyolite flows from drill hole WKP-18 at 311-m depth. Adularia extracted from vein to obtain ^{40}Ar/^{39}Ar dates.